Journal of
Water & Climate Change

 Journal of Water and Climate Change Vol 16 No 11, 3372 doi: 10.2166/wcc.2025.097

# A remote sensing approach for characterizing lake responses to heatwaves and monsoons: a case study from India

Rossana Caroni [a], Anna Joelle Greife [a,b], Mariano Bresciani [a], Claudia Giardino [a], Marina Amadori [a] and Monica Pinardi [a,*]

[a] Institute for Electromagnetic Sensing of the Environment, National Research Council, Via Corti 12, 20133, Milan, Italy
[b] Department of Environmental Science and Policy, University of Milan, Via Giovanni Celoria 2, 20133 Milan, Italy
*Corresponding author. E-mail: pinardi.m@irea.cnr.it

RC, 0000-0003-1891-6319; AJG, 0009-0009-4152-9473; MB, 0000-0002-7185-8464; CG, 0000-0002-3937-4988; MA, 0000-0001-8810-8478; MP, 0000-0001-5289-8842

## ABSTRACT

The timing and intensity of monsoons strongly regulate the Indian subcontinent's climate, shaping water quality and availability. In 2019, a delayed monsoon following an exceptional heatwave offered a unique case to assess lake responses to climatic extremes. We analyzed satellite-derived lake turbidity and chlorophyll-a data from 42 lakes and reservoirs across the region. Our approach combined time alignment measurement analysis, cross-correlation, and clustering to investigate the main drivers of variability. Results showed that monsoon precipitation was the main driver of turbidity dynamics. Turbidity time series were more closely aligned with precipitation and air temperature, and cross-correlation analysis indicated a consistent 1-month lag between cumulative precipitation and turbidity. Available lake water level data confirmed that large fluctuations can occur within short timescales, strongly influencing water quality. Cluster analysis of annual turbidity and chlorophyll-a patterns provided insights into lake responses to heatwaves and monsoon periods. Turbidity cluster patterns largely followed precipitation patterns, whereas chlorophyll-a clusters reflected the influence of lake morphology, phytoplankton dynamics, and interactions with turbidity changes. Overall, our findings highlight the strong dependence of lake water quality on monsoon dynamics and emphasize the potential of remote sensing for monitoring and adaptive management in a changing climate.

**Key words:** chlorophyll-a, heatwave, lakes, monsoon, satellite data, turbidity

## HIGHLIGHTS

- Potential compound responses of lake water quality to heatwaves and monsoon events were investigated using satellite data.
- Monsoon precipitation was the main driver of water turbidity dynamics.
- High variation in lake water level was related to changes in water quality.
- Lake chlorophyll-a patterns were complex and more related to individual lake characteristics and additional anthropogenic pressures.

## 1. INTRODUCTION

The occurrence of extreme climatic events, such as heatwaves and storms, is predicted to increase in frequency, intensity and duration (Seneviratne *et al.* 2021; You & Wang 2021; Shaw *et al.* 2022; Sauter *et al.* 2023; Yang & Yuan 2025), becoming a concerning issue in both ecological research and in the global change agenda. Recent research has shown that the frequency, severity and duration of heatwaves have significantly increased in many parts of the world, including Europe (Dosio & Fisher 2018), North America (Habeeb *et al.* 2015; Meehl & Tebaldi 2004), Australia (Perkins & Alexander 2013) and Asia, spanning from Middle East (Rezaee *et al.* 2025) to East Asia (Ding *et al.* 2010), consistent with the growing impacts of climate change globally (Perkins-Kirkpatrick & Lewis 2020). There is general agreement that changes in the frequency and severity of extreme climate events and in the variability of weather patterns will have significant consequences for human and natural systems (Thornton *et al.* 2014). Increasing frequencies of heat stress, drought and flooding events are projected for the rest of this century and it is likely that anthropogenic influence has significantly increased the probability of occurrence of heatwaves (IPCC 2013). Air temperature heatwaves can induce lake heatwaves, which are periods of unusually warm surface water, impacting thermal structure and ecosystem processes (Woolway *et al.* 2021). Summer heatwaves can affect lake ecosystems, potentially altering species and community composition (Rasconi *et al.* 2017), pushing lake ecosystems to their resilience limit (Woolway *et al.* 2021) and resulting in changes in aquatic food webs. Common severe consequences include phytoplankton blooms (Joehnk *et al.* 2008) and mass fish die-off events (Till *et al.* 2019). Over time, an increase in the exposure of lake ecosystems to hot temperature extremes may lead to an irreversible loss of species as already observed in the oceans due to the increased frequency of marine heatwaves (Smale *et al.* 2019; Straub *et al.* 2019). Intense and prolonged heatwaves can also reduce the ecological services that lakes provide, such as the provision of safe water for drinking and agricultural irrigation, recreational uses, and economic benefits like fisheries and tourism, all negatively impacting local economies and threatening health conditions (Caretta *et al.* 2022; Parmesan *et al.* 2022; Woolway *et al.* 2022a). Despite a rising awareness of their importance, the scientific understanding of lake heatwaves is still at the beginning (Woolway *et al.* 2022b).

Rapid changes in temperature and weather conditions can also have ecological implications (e.g., You & Wang 2021). Passing from extremely high temperatures occurring during heatwaves to sudden temperature declines brought by low-pressure conditions can pose a potential threat to lake ecosystems (Free *et al.* 2022). The occurrence of cold and cloudy systems leading to drops in temperature and periods of low irradiance can disrupt lake metabolism, particularly in eutrophic shallow lakes, leading to a rapid decline in primary production and significantly negative net ecosystem production, lowering oxygen concentrations and can lead to fish kills (Jeppesen *et al.* 2021). Moreover, when low-pressure conditions are accompanied by precipitation, the impact directly on the lake surface and through the catchment runoff can be severe, with increased input of material and nutrients leading to increased lake turbidity, with subsequent potential influence on phytoplankton dynamics (Stockwell *et al.* 2020). Northern Hemisphere monsoon precipitation has recently shown increasing trends (Collins *et al.* 2024), although the main drivers remain unclear (Huang *et al.* 2020).

With a population of 1.3 billion, India is one of the hot spots experiencing severe heatwaves, which generally occur during May–June (https://www.dataforindia.com/population-growth/; Hari *et al.* 2022). Since the beginning of the century, a significant increase in the number of mega heatwaves has been recorded for the Indian subcontinent (Rohini *et al.* 2016; Vittal *et al.* 2020a; Hari *et al.* 2022). The occurrence of heatwaves over India is mostly associated with high-pressure systems characterized by anticyclonic wind patterns and sinking air which prevents cloud formation, with subsequent clear sky conditions, intense surface heating and decreased soil moisture (Ratnam *et al.* 2016; Zore *et al.* 2021). The recent deadly heatwaves of 2015 and 2019 claimed more than 1,200 lives for heat exhaustion, dehydration, and heatstroke (Dunn *et al.* 2020; Dube *et al.* 2021). The 2019 heatwave, one of India's longest and most intense heatwaves in decades, occurred from mid-May to mid-June (Indian Meteorological Department 2020) and air temperatures reached 51 °C in Rajasthan, Northern India, which is considered the region with the highest risk of heatwaves in the country (Vittal *et al.* 2020b). The year 2019 was registered as one of the warmest in India since 1901 (India Meteorological Department 2020), with an overall mean air temperature 0.36 °C above the annual average, with hot and dry conditions recorded. Many countries in Africa, Europe, Asia, and Australia also reported record high annual air temperatures, and lake temperatures increased on average across the globe in 2019 (NOAA 2019). After the 2019 intense long heatwave, India experienced one of its heaviest summer monsoon rains (starting from late June) since 1995 (Dunn *et al.* 2020). June is a crucial month in India, as the region awaits the arrival of monsoons which bring relief from the heatwaves during the drier pre-monsoon season. The population of the Indian subcontinent strongly relies on the water supply from the Indian summer monsoon (Singh *et al.* 2019), as it provides about 80% of the annual rainfall to South Asia and is the strongest component of the global monsoon system (Jin & Wang 2017). Monsoon rainfalls induce air temperature cooling (Zhou *et al.* 2019), replenish freshwater ecosystems and recharge water reservoirs. A slight delay in monsoon onset dates (5–7 days) could cause more severe and long-lasting heatwaves.

A positive trend in Indian summer monsoon rainfall was clearly detected in satellite-based estimates and *in situ* observations between 2002 and 2014 (Jin & Wang 2017). Such a revival of the Indian summer has been attributed to enhanced land-sea temperature contrast due to the accelerated warming of the Indian continent compared to the tropical Indian Ocean (Roxy 2017). However, the Indian Ocean dipole also influences the intensity of the Indian Summer monsoon rains. In October 2019, the Indian Ocean dipole exhibited its greatest magnitude since 1997, with anomalous warming of the Western Indian Ocean and cooling in the Eastern Indian Ocean (Blunden & Arndt 2020). The increasing frequency and intensity of extreme climate events, such as heatwaves and floods, are among the most expected and recognized consequences of climate change. Prediction of water quality parameters becomes a challenging task with these extremes since water quality is strongly related to hydro-meteorological processes and sensitive to climate change (Fabian *et al.* 2023).

The aim of this study is to investigate the potential effects of heatwaves and monsoon rainfalls of water quality parameters for major Indian lakes from Earth Observation (EO) data.

Satellite remote sensing is an important climate system, as it allows for observing the state of key variables across land, ocean and atmosphere, and their evolution at different spatio-temporal scales (Yang *et al.* 2013; Zhao *et al.* 2023). EO data are also widely used to support policy makers by providing observations for the development of prevention, mitigation and adaptation measures to face the impacts of climate change (Joyce *et al.* 2009; Kansakar & Hossain 2016). The detection of large-scale climate extremes such as floods and droughts, by means of EO data, allows to map changes in both water quality and quantity (e.g., Jiao *et al.* 2021; Albertini *et al.* 2022), and resilience of aquatic ecosystems. To better characterize the response of water quality to extreme climate events, it is important to have accurate and long-term climate and water quality data (Fabian *et al.* 2023).

Using an open-source EO dataset of globally consistent satellite observations of the essential climate variable “Lakes”, key water quality components, such as Chlorophyll-a concentration (Chl-a) and turbidity, were analyzed across aquatic systems on the Indian subcontinent for the period 2017–2020. Particularly, a focus on the potential response of water quality to heatwaves and monsoon rainfalls in 42 Indian lakes covering different climatic and ecological settings in the year 2019 is presented. By investigating the compound effects of extreme climatic events such as heatwaves and monsoon rainfalls, this study provides novel insights into the drivers and responses of lake ecosystems which play a crucial role in delivering essential ecosystem services across the entire region. Our research addresses key international goals related to climate change and hydrology, highlighting the urgency of coordinated actions to safeguard freshwater ecosystems under a changing climate.

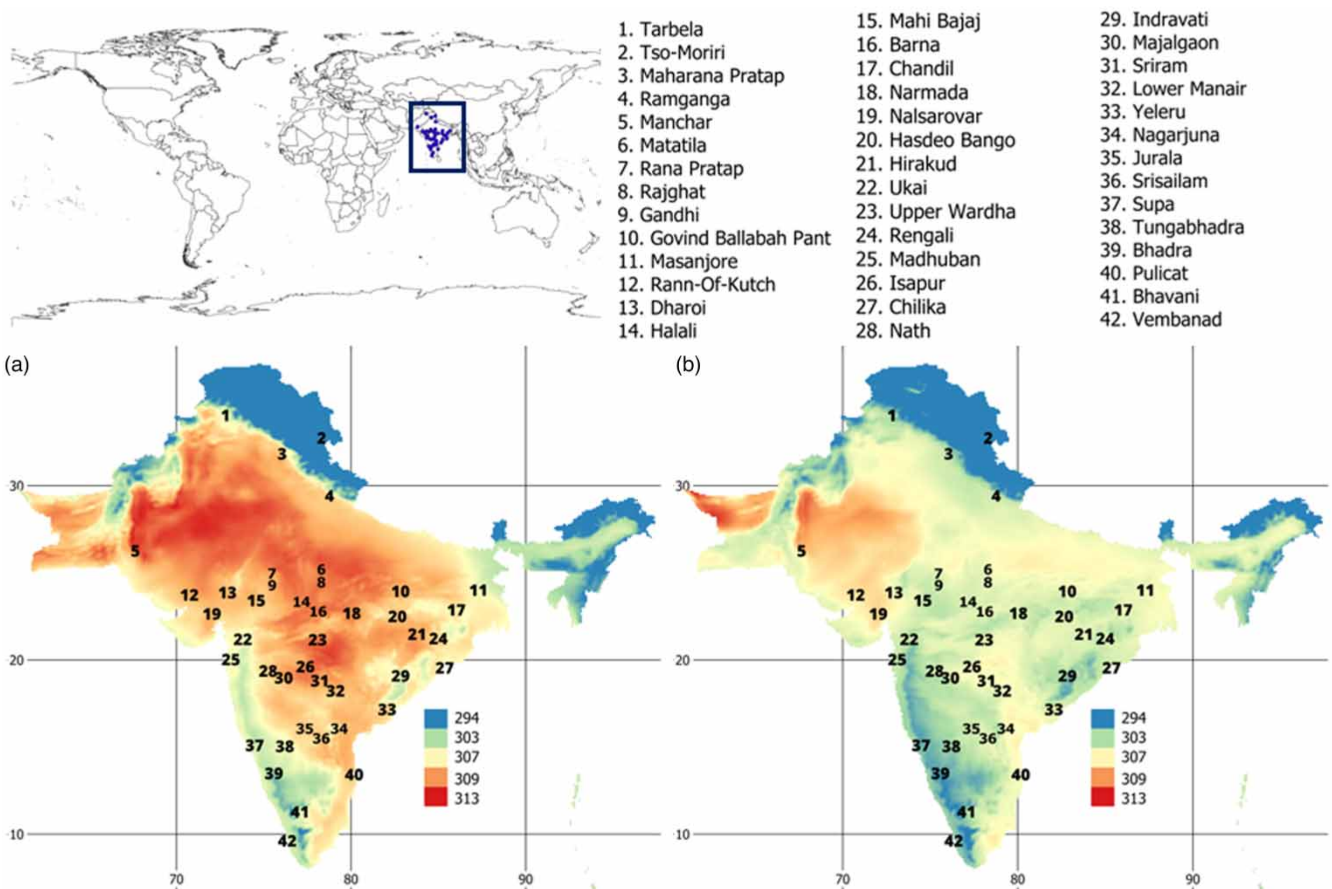


**Figure 1** | Maps of India subcontinent with the selected lakes distribution and air temperature (Kelvin) on 1 June 2019, i.e., during the heatwave period (a) and 18 July 2019, i.e., during the monsoon period (b).

## 2. MATERIAL AND METHODS

### 2.1. Study area

This study focused on 42 large lakes across the Indian subcontinent, all included in the Lakes_cci dataset. The spatial distribution of these lakes is shown in Figure 1, overlaid on maps of air temperature during the 2019 heatwave (Figure 1(a)) and monsoon (Figure 1(b)) periods. The lakes are located in the region extending from 10°N to 34°N, from 70° E to 87° E, hence representing significant latitudinal and longitudinal gradients across multiple ecoregions, from humid subtropical to arid to highlands. The lake types are mainly reservoirs (33), with only 9 natural lakes.

Land cover (LC) categorization (Figure 2(a)) revealed that most lakes ($n = 25$) had croplands (either rainfed or irrigated) in their catchments, mainly located in central India. In the rest of the country, lake catchments displayed a mosaic of trees and shrubs, with only six lakes having their catchment covered prevalently by trees. Most of the lakes are located in regions classified as tropical, savannah and monsoon ($n = 21$), and the remaining lakes are included in temperate, dry winter, hot summer regions ($n = 11$) and in arid, hot regions ($n = 9$) (Figure 2(b)). Figure 3 shows lake area, average depth and elevation. Lakes

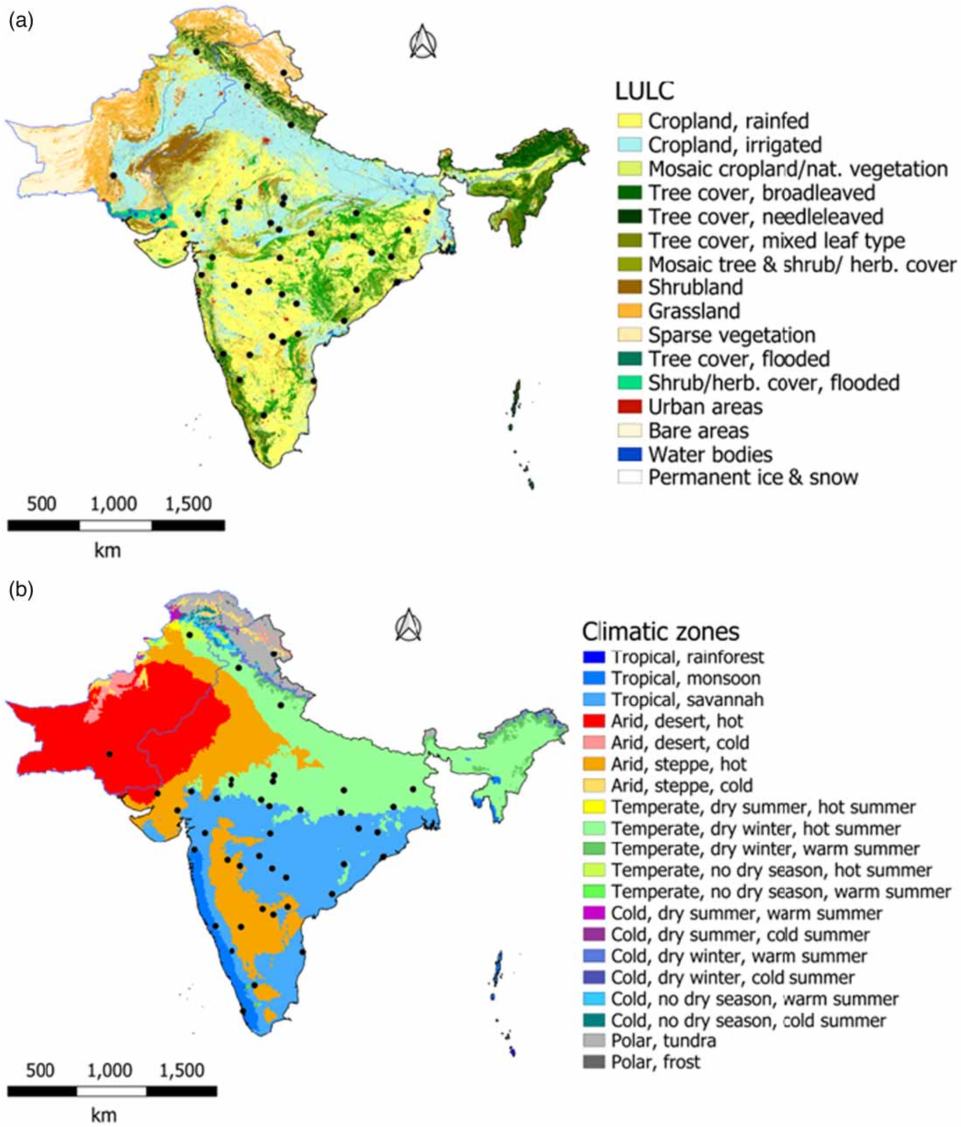


**Figure 2** | Thematic maps of India (dark line) and Pakistan (blue line) with CCI lakes showing lake catchment land cover (LC) of the lake catchment (a); climatic zones classification (b).

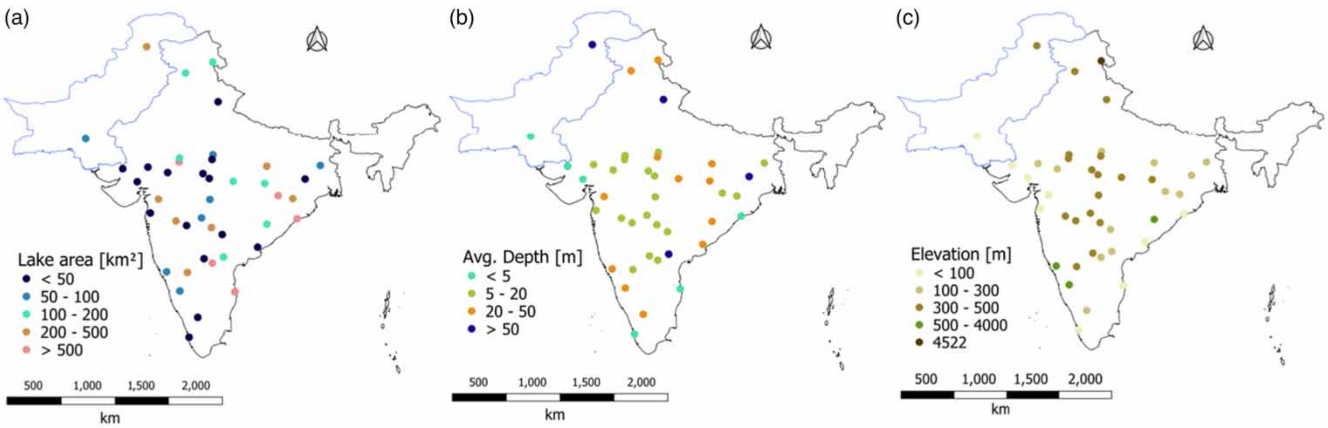


**Figure 3** | Thematic maps of India (dark line) and Pakistan (blue line) with CCI lakes showing lake area (km$^2$) (a); lake average depth (b); lake elevation (m a.s.l.) (c).

were categorized as relatively small (<50 km$^2$, $n = 16$) and large (between 50 and 500 km$^2$, $n = 20$), with five very large lakes having a surface area >500 km$^2$ (Figure 3(a)). Lakes largely fell into three groups by mean depth, shallow (<5 m; $n = 6$), medium (5–20 m; $n = 20$) or deep (>20 m; $n = 16$), including four very deep lakes (>50 m; $n = 4$) (Figure 3(b)). The lakes are mainly located at hills altitude (300–500 m asl; $n = 17$), followed by lakes at lower altitudes between 100 and 300 m asl ($n = 12$) and lakes in lowlands (<100 m asl; $n = 9$), with few lakes ($n = 4$) at highest altitudes (between 700 m asl and one at 4,522 m asl) (Figure 3(c)).

## 2.2. Datasets

In this study, we utilized several datasets widely referenced in the literature that guarantee global coverage. In Table 1, we report a summary of all variables used along with their spatial and temporal resolution, their respective source dataset and its official reference.

### 2.2.1. Satellite data: water quality and water level

The Lakes_cci project, funded by the European Space Agency (ESA) in the Climate Change Initiative, provides an open-source EO dataset of globally consistent satellite observations of the essential climate variable "Lakes" which includes Chl-a and turbidity products, along with other lakes variables, as lake water level (LWL) and extent, surface water temperature and ice cover and thickness. The dataset builds on multi-mission satellite data for 2024 lakes for the period 1992–2022 in a common grid with a 1/120° latitude-longitude resolution (Carrea *et al.* 2023).

We selected the Lakes_cci dataset as it is a recent and under-explored dataset with high potential due to its long-term data and global coverage.

Relevant for this study, are the Lakes_cci products (v2.1) of Chl-a and turbidity available for the 42 lakes. These products are generated from Sentinel-3 Ocean and Land Colour Instrument (OLCI) via the Calimnos v1.4. processing chain. It combines several functionalities as radiometric and atmospheric corrections; the latter performed with POLYMER v4.13 and optical water type classification (Simis *et al.* 2023). This classification is then used to apply the algorithms for retrieving Chl-a and turbidity, as described by the tuning techniques in Neil *et al.* (2019).

The Lakes_cci LWL products, which are only available for seven out of 42 lakes, used to support the water quality analysis, were derived from radar altimetry observations collected by Poseidon-3 (Jason-2), Poseidon-3B (Jason-3), and the SAR altimeter onboard Sentinel-3 over the study period. Altimetric heights and their associated uncertainties were computed following the methodologies described in Carrea *et al.* (2023) and Crétaux & Birkett (2006). All the satellite-derived variables in the Lakes_cci dataset are provided with related uncertainties, while the quality of the retrieved Chl-a, turbidity and LWL products is assessed by comparison with independent *in situ* measurements (Carrea *et al.* 2023).

From this dataset, we considered variables for the period 2017–2020 (Table 1), which was selected both to ensure consistent coverage from Sentinel-3 OLCI and to provide a medium-term context around the 2019 target year. For the analysis, Chl-a and turbidity from 42 lakes were considered. These variables are available as time series of maps. We selected valid pixels in

**Table 1** | Description of the source and resolution of the datasets used in this study

| Category | Variable | Product | Source | Time step | Reference |
|---|---|---|---|---|---|
| Water quality | Chlorophyll-a | Lake Water Leaving Reflectance (LWLR) – ESA Lakes_cci v2.1 | Sentinel-3 (2016–2020), 300 m–1 km | Daily, 2017–2020 | Carrea *et al.* (2023) |
| | Turbidity | Lake Water Leaving Reflectance (LWLR) – ESA Lakes_cci v2.1 | Sentinel-3 (2016–2020), 300 m–1 km | Daily, 2017–2020 | Carrea *et al.* (2023) |
| Water level | Water level | Lake Water Level (LWL) – ESA Lakes_cci v2.1 | Sentinel-3 (2016–2020), 300 m–1 km | Daily, 2017–2020 | Carrea *et al.* (2023) |
| Morphological | Lake surface area | HydroLAKES (v1.0) | HydroSHEDS | Temporal snapshot | Messager *et al.* (2016) |
| | Length of shoreline | HydroLAKES (v1.0) | HydroSHEDS | Temporal snapshot | Messager *et al.* (2016) |
| | Shoreline development Total lake or reservoir volume | HydroLAKES (v1.0) | HydroSHEDS | Temporal snapshot | Messager *et al.* (2016) |
| | Average lake depth | HydroLAKES (v1.0) | HydroSHEDS | Temporal snapshot | Messager *et al.* (2016) |
| | Average long-term discharge flowing through the lake | HydroLAKES (v1.0) | HydroSHEDS | Temporal snapshot | Messager *et al.* (2016) |
| | Average residence time of the lake water | HydroLAKES (v1.0) | HydroSHEDS | Temporal snapshot | Messager *et al.* (2016) |
| | Elevation of lake surface | HydroLAKES (v1.0) | HydroSHEDS | Temporal snapshot | Messager *et al.* (2016) |
| | Average slope within a 100 m buffer around the lake polygon | HydroLAKES (v1.0) | HydroSHEDS | Temporal snapshot | Messager *et al.* (2016) |
| | Area of the watershed associated with the lake | HydroLAKES (v1.0) | HydroSHEDS | Temporal snapshot | Messager *et al.* (2016) |
| Catchment type | Lake catchment | Lake-TopoCat | HydroLAKES v1.0; MERIT Hydro v1.0.1; MERIT Hydro-Vector; Global Lake area, Climate, and Population (GLCP) database. | – | Sikder *et al.* (2023) |
| Climate type | Climate classification | Köppen-Geiger climatic zones | Resampled Köppen-Geiger maps – 0.01° | Temporal snapshot | Beck *et al.* 2023 |
| Land surface characteristics | Land cover | ESA CCI Landcover dataset (v2.1.1) | Sentinel-3 – 300 m | Annual - 2019 | Defourny *et al.* 2023 |
| Meteo-climatic | 2 m air temperature (t2 m) | ERA5-Land | Modelled data, 11 km | Daily aggregated, 2017–2020 | Muñoz Sabater 2019 |
| | Total precipitation (tp) | ERA5-Land | Modelled data, 11 km | Daily aggregated, 2017–2020 | Muñoz Sabater 2019 |

these maps by applying uncertainty thresholds of 60% (Chl-a) and 70% (turbidity), following previous studies that indicated such thresholds as optimal to balance data quality and sample size (Free *et al.* 2022; Pinardi *et al.* 2023). LWL data, available for seven lakes in the Indian subcontinent (namely Maharana Pratap n. 3, Gandhi n. 9; Govind Ballabah Pant n. 10; Hirakud n. 21; Chilika n. 27; Nath n. 28; Srisailam n. 36; the numbers refer to the lakes shown in Figure 1) were included in the study after being filtered for an uncertainty lower than 30%. Daily mean values of Chl-a, turbidity and LWL per single lake were calculated by spatially averaging all valid pixels.

The trophic status of the selected 42 lakes, based on the annual mean Chl-a concentration for the period 2017–2020, was calculated according to the following classification (OECD 1982): oligotrophic <2.5 mg m$^{-3}$; mesotrophic from 2.5 to 8 mg m$^{-3}$; eutrophic between 8 and 25 mg m$^{-3}$; hypertrophic >25 mg m$^{-3}$.

#### 2.2.2. Morphological data

Information regarding lakes and their catchment areas was gathered from the HydroLAKES dataset (Messager *et al.* 2016). HydroLAKES, available for lakes with a surface area of at least 10 ha, provided attribute details for the 42 lakes studied, including parameters such as surface area, shoreline length, total volume, mean depth, discharge rates, residence time, elevation, and geographical coordinates (Table 1). The list of lakes with the main hydro-morphological characteristics is presented in Table S1 in the supplementary material.

#### 2.2.3. Catchment type

Lakes were also classified based on the climatic and anthropogenic characteristics of their catchment, defined as the unit catchments ("Catchments_pfaf_45") assigned to each lake in the Lake-TopoCat dataset (Sikder *et al.* 2023) (Table 1).

#### 2.2.4. Climate-type and land surface characteristics

In particular, we considered the catchment climate zone after the modified Köppen–Geiger climatic zones (Beck *et al.* 2023), and its dominant LC, as obtained from the global LC maps at 300 m spatial resolution, provided on an annual basis from 2016 to 2020 (Defourny *et al.* 2023) (Table 1).

#### 2.2.5. Meteo-climatic data

Climatic data of air temperature (2m_temperature) and total precipitation (total_precipitation_sum) at a daily resolution for the period 2017–2020 were obtained for each lake catchment from ERA5 Land (Muñoz-Sabater et al. 2021) (Table 1). Air temperature was used in the analysis as it provides a more responsive indicator of heatwave dynamics than lake temperature, which can be slow to respond owing to thermal inertia (Woolway *et al.* 2021).

With respect to precipitation, it is widely recognized that the total precipitation product of ERA5 reanalysis has varying performances depending on the geographic location and the specific meteorological single events being observed. In our work, we relied on the validation performed provided by dedicated investigations in India (Singh *et al.* 2023, Kumar *et al.* 2024), which assessed the accuracy of reanalysis products, including ERA5, in comparison with *in situ* measurements. Singh *et al.* (2023) reported that ERA5 tends to underestimate rainfall intensity in mountainous and hilly regions. Kumar *et al.* (2024) noted limitations in ERA5's ability to capture the timing and the intensity of extreme events such as lightning. Nevertheless, ERA5 is generally recognized as reliable for analyses on broader temporal scales, such as seasonal or interannual variability (Singh *et al.* 2023), which aligns with the objectives of our medium-term analysis for the 2017–2020 period. Regarding the specific case of the 2019 heatwave and subsequent monsoon season, we further cross-checked ERA5 cumulative precipitation estimates with those reported by the Indian Meteorological Department in its annual report (IMD 2020), finding a satisfactory level of consistency for the monsoon season (June–September).

### 2.3. Statistical analyses

#### 2.3.1. General statistical analysis

Statistical analysis (regression, correlation, Analysis of Variance (ANOVA)) and visualization of the data were carried out with R (Wickham 2016; R Core Team 2021; Soetaert 2021). The time series of air temperature, precipitation, Chl-a and turbidity were smoothed via a LOWESS (Locally Weighted non-parametric Smoothing) line using a span of 10% of the dataset and a window half-width of 5 days, chosen to preserve temporal trends considering the overpass frequency of Sentinel-3. This ensured that a sufficient number of days were included in the smoothing window, producing a representative smoothing curve. The method allowed peak identification by detecting local maxima through the R package zoo (Zeileis *et al.* 2022).

Missing daily values of Chl-a and turbidity were linearly interpolated, consistent with classical approaches in handling satellite-derived timeseries satellite data (Amadori *et al.* 2024). Such gap-filling does not alter the maximum value detected but may reduce the accuracy of the results, as higher local maxima might have occurred in the missing dates.

### 2.3.2. Time alignment measurement

In order to quantify the degree to which time series of air temperature, precipitation, lake Chl-a and turbidity were temporally aligned we carried out a TAM for each lake during 2019 and also during the period 2017–2019 (Folgado *et al.* 2018). Such analysis was performed on smoothed timeseries normalized by their respective maximum value. TAM values range from 0 to 3, with 0 indicating perfect temporal alignment between the timeseries, and 3 indicating complete misalignment.

### 2.3.3. Cluster analysis

Annual pattern analysis of Chl-a and turbidity was performed for 2019 for each lake, identified by fitting a LOWESS line. A hierarchical cluster analysis was carried out using the Euclidean distance with Wards minimum variance method (Szekely & Rizzo 2005) to identify and aggregate similar lake types in terms of Chl-a and turbidity patterns. The dendrograms were cut at an indicated number of groups based on the silhouette method to compare similarity within and among clusters (Kassambara & Mundt 2017; Maechler *et al.* 2024). The dataset for cluster analysis was reduced to 39 lakes for Chl-a and to 37 lakes for turbidity for analysis due to gaps in the time series. ANOVA was carried out on each identified cluster to compare Chl-a concentrations and turbidity in selected time intervals (pre-heatwave DOY 50–110; during heatwave DOY 111–170; post-heatwave/start monsoon DOY 171–230; monsoon season DOY 231–340).

### 2.3.4. Cross-correlation analysis

In order to investigate correlations between time series, we performed a cross-correlation analysis between monsoon cumulative rainfall (30 days) and turbidity values during 2019. The period of 30 days was selected as dynamic changes in parameters could be detected. The cross-correlation analysis was run using the forecast package (Hyndman & Khandakar 2008) in R on pre-processed data to improve stationarity and harmonize residuals (differenced and whitened).

## 3. RESULTS

### 3.1. Lake characteristics

Based on mean lake Chl-a concentrations, the trophic status of the selected lakes was calculated. This revealed a dominance of eutrophic conditions ($n = 33$), with the remaining lakes exhibiting mesotrophic ($n = 6$) or hypertrophic conditions ($n = 3$).

Regarding the general climatic patterns, interannual variability of air temperature (°C) and precipitation (total precipitation m) showed similarities between 2017 and 2020. In all lakes, air temperature increased from January to May–June, which corresponds to the dry season when maximum annual values were reached, followed by a drop in June, in relation to the arrival of the monsoon rains (Figures 4(a) and 4(b)).

The mean annual turbidity for the period 2017–2020 ranged from 2.0 to 69.3 NTU for all lakes in the study. Lakes with the highest annual turbidity were Rengali (n. 24; 25 NTU), Indravati (n. 29; 38 NTU) and Kutch (n. 12; 51 NTU). Turbidity values generally rose during the rainy season (July-September), although with diverse magnitude (Figure 4(c)). The mean annual Chl-a for the period 2017–2020 ranged from 3.4 to 57.5 mg $m^{-3}$ considering all lakes. Lakes with the highest annual Chl-a concentration were Sriram (n. 31), Halali (n. 14), Bhavani (n. 41) and Nalsarovar (n. 19) with values above 20 mg $m^{-3}$. Chl-a showed various patterns across lakes, often not directly linked to a clear seasonal behavior (Figure 4(d)).

### 3.2. TAM analysis

TAM analysis was performed comparing paired time series during 2019 and during the 4-year period 2017–2020 in the following combination: total precipitation to air temperature, to turbidity and to Chl-a; turbidity to Chl-a; air temperature to Chl-a and to turbidity. Table 2 reports the results of the analysis conducted separately on the time series of 2019 and on the 4-year period 2017–2020.

The time series of precipitation was closer in phase with the time series of turbidity (mean value of 2.26 and 1.99 for 2019 and 2017–2020, respectively), while less in phase with Chl-a (mean value of 2.67 and 2.21 for 2019 and 2017–2020, respectively) (significant difference *t*-test $p < 0.001$). The time series of air temperature had the best fit with precipitation (mean value of 1.64 and 1.53 in 2019 and 2017–2020, respectively).

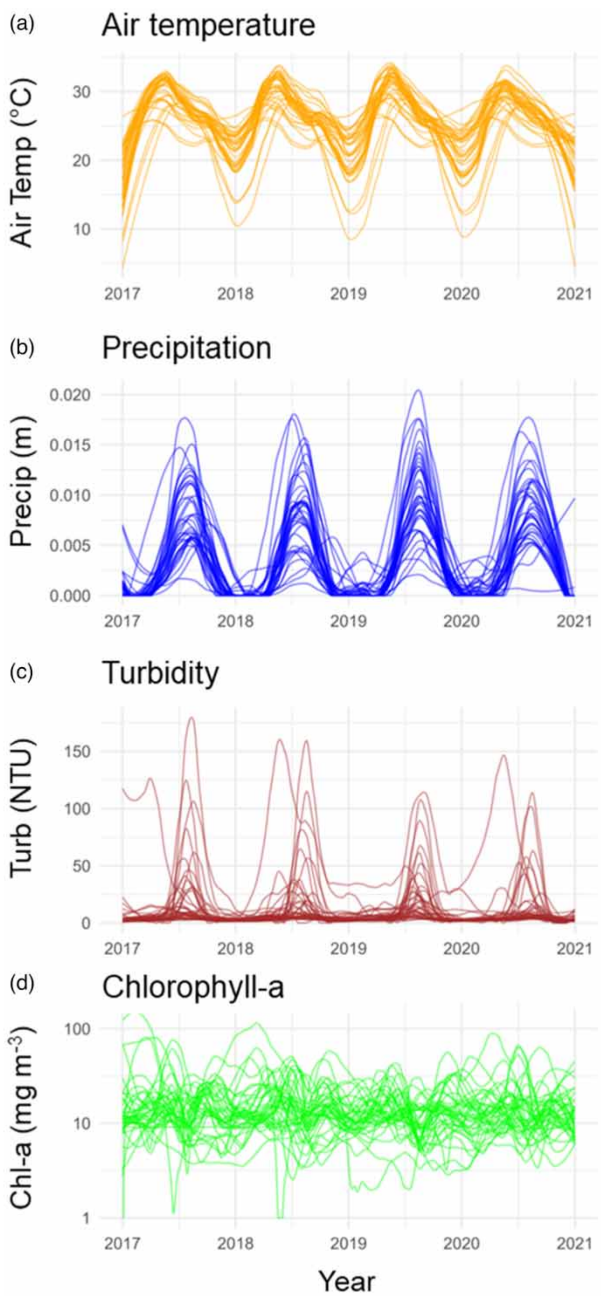


**Figure 4** | Interannual patterns of air temperature (°C) (a), total precipitation (m) (b), turbidity (NTU), (c) and chlorophyll-a (mg $m^{-3}$) (d) for the studied Indian lakes during the period 2017–2020. Each line corresponds to the LOWESS smoothed timeseries for one lake.

### 3.3. Cluster analysis

Cluster analysis was performed with annual patterns of Chl-a concentrations and turbidity in 2019 for each of the studied lakes. Figure 5 reports the clusters of lakes obtained from the analysis of Chl-a and turbidity timeseries as identified via the Silhouette test (Figure S1 in Supplementary Material). For each cluster, we also report the annual pattern characterizing each cluster for both variables in Figure 6.

Three main clusters were identified for Chl-a concentration by cluster analysis and Figure 6(a) shows the Chl-a annual patterns (relativized to the mean) for each cluster. When Chl-a clusters were compared to the hydro-morphological variables of the related lakes, differences among the clusters were not statistically significant ($p > 0.05$) with any of the variables tested.

**Table 2** | Results of the TAM (time alignment measurement) analysis for the year 2019 and for the period 2017–2020

| | 2019 | | | 2017–2020 | | |
|---|---|---|---|---|---|---|
| **TAM** | **Mean** | **Median** | **StdDev** | **Mean** | **Median** | **StdDev** |
| prec_turb | 2.26 | 2.37 | 0.13 | 1.99 | 2.01 | 0.17 |
| prec_Chl-a | 2.67 | 2.67 | 0.12 | 2.21 | 2.22 | 0.13 |
| turb_Chl-a | 2.63 | 2.67 | 0.13 | 2.18 | 2.14 | 0.19 |
| turb_airT | 2.45 | 2.42 | 0.12 | 1.98 | 1.94 | 0.18 |
| Chl-a_airT | 2.69 | 2.71 | 0.09 | 2.12 | 2.10 | 0.16 |
| prec_airT | 1.64 | 1.64 | 0.21 | 1.57 | 1.53 | 0.17 |

Prec, total precipitation (m); airT, air temperature (C°); turb, turbidity (NTU); Chl-a, chlorophyll-a (mg $m^{-3}$).

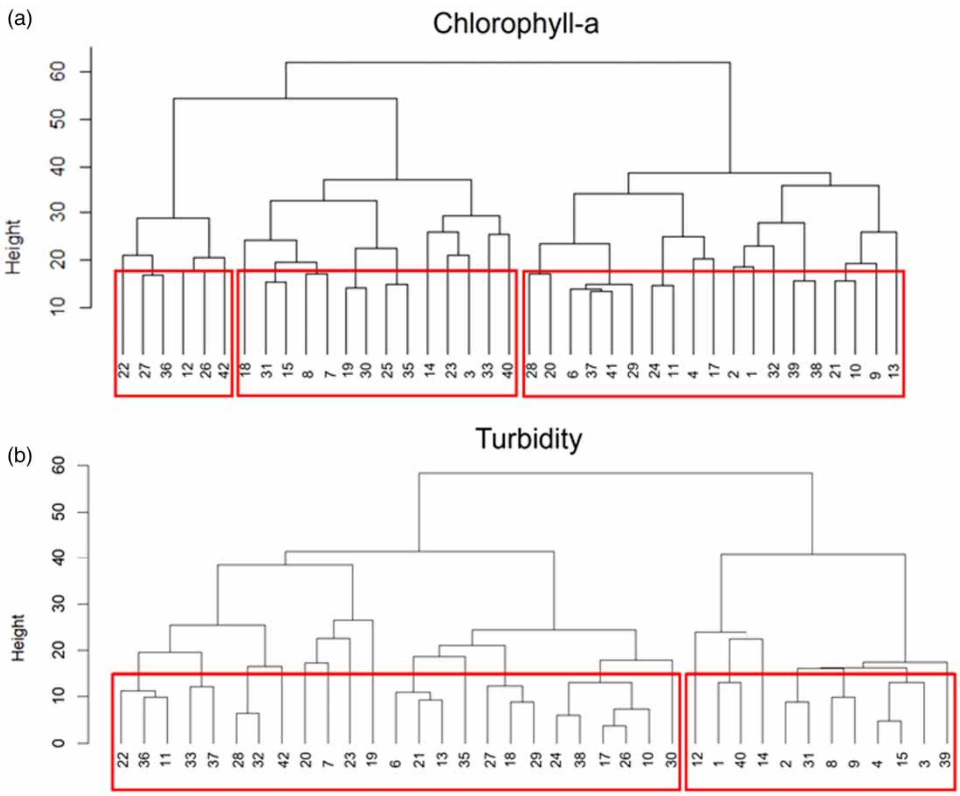


**Figure 5** | Dendrograms of the results of cluster analysis for lake chlorophyll-a (a) and turbidity (b) patterns in Indian lakes. The numbering refers to the lake identifiers in Figure 1.

However, we observed that clusters tend to group lakes similar in depth and lake area, with cluster 1 having generally larger and shallower lakes, cluster 2 deeper lakes and cluster 3 including small lakes.

Two main clusters were identified for turbidity by cluster analysis, and Figure 6(b) shows the turbidity annual patterns (relativized to the mean) for each cluster. When turbidity clusters were compared with the hydro-morphological variables of the related lakes, a significant difference was found between turbidity patterns and lake latitude (2-sample *t*-test, $p < 0.05$), with lakes in cluster 2 located at significantly higher latitude than lakes in cluster 1.

Cluster analysis performed on Chl-a patterns resulted in three main clusters (Figure 6(a); Figure S1) where a different behavior of the Chl-a timeseries was observed during the two phases of heatwave and monsoon (Figure 6(a)). During the heatwave, Chl-a either decreased (cluster 1; $n = 6$), increased (cluster 2; $n = 14$) or remained quite unchanged (cluster 3;

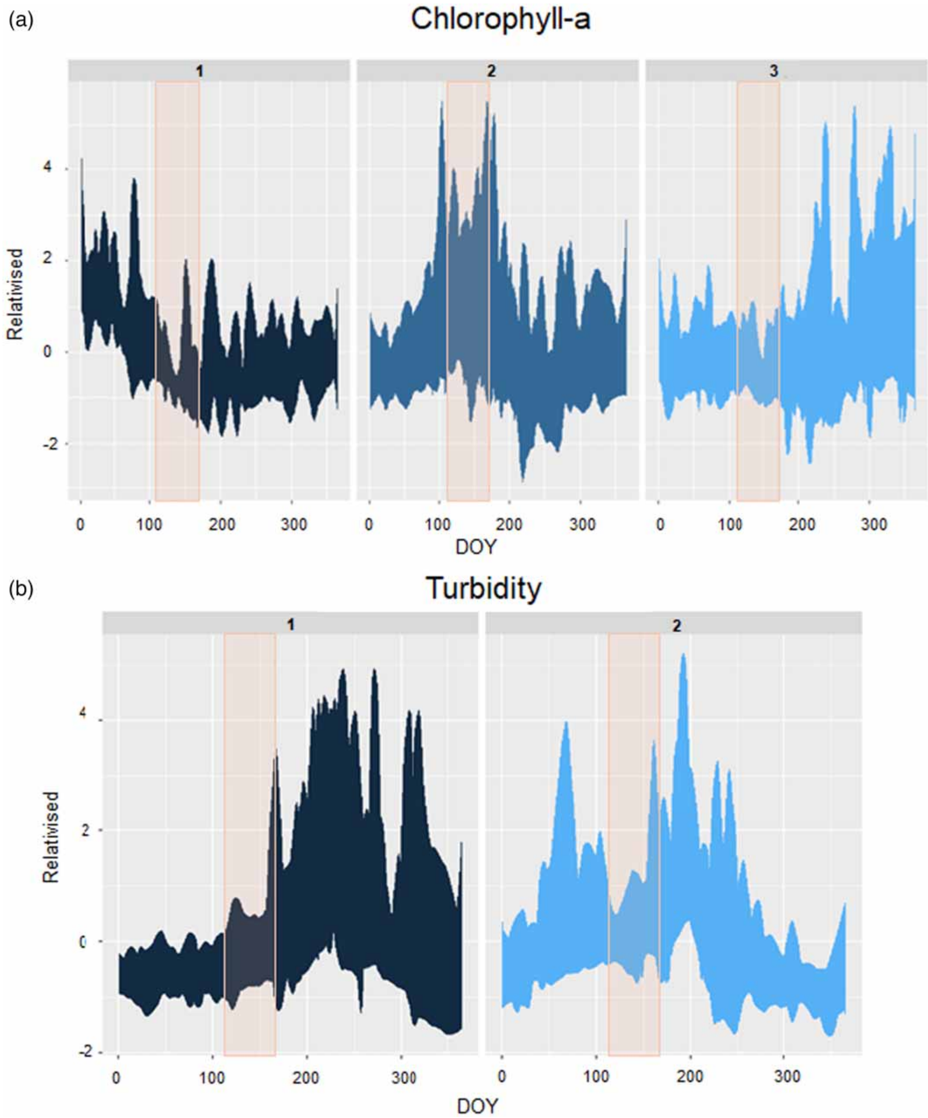


**Figure 6** | Lake chlorophyll-a (a) and turbidity (b) (relativized) patterns by cluster; transparent boxes indicate the heatwave period (DOY 111–170).

$n = 19$). When focusing on the latest period of the year, after the monsoon season, only lakes in cluster 3 showed a remarkable increase in Chl-a. Regarding lake morphological characteristics, cluster 1 included mainly large (median of lake area = 227 km$^2$) and shallower (median of average depth = 8.9 m) lakes, while cluster 3 included smaller (median = 46 km$^2$) and medium depth (median = 12.0 m) lakes and cluster 2 deep lakes (median = 21 m). The LC for cluster 1 and cluster 3 were mainly cropland (80 and 62%, respectively) and cluster 2 was more diverse, including cropland (60%), tree cover (33%) and grassland. Lakes in cluster 1 were mainly located in tropical climate zones, while those of cluster 2 were mainly found in temperate areas, and one in polar climates.

Cluster analysis performed on turbidity revealed two main clusters (Figure 5(b); Figure S1 in Supplementary Material). Lakes of cluster 1 show a unimodal pattern of turbidity, while a bimodal pattern is shown for cluster 2 (Figure 6(b)). In cluster 1, the turbidity peak between DOY 210 and 250 followed mainly the monsoon rain extent and amount. The bimodal pattern of cluster 2, which includes lakes located at significantly higher latitudes, can be explained by snow melting processes favoring the first turbidity peak (at DOY around 80) while the second turbidity peak is likely due to monsoon rains. During the latest period of the year, cluster 2 showed a steeper decline in turbidity in comparison to cluster 1 and reached lower values, likely due to snow presence in this period. The LC in cluster 1 was mainly cropland, both rainfed and irrigated, while cluster 2 was more diverse but dominated by rainfed cropland. As for climate zones, cluster 1 was a mix with dominance of tropical monsoon, followed by temperate and arid steppe, while cluster 2 showed mostly temperate and tropical savannah climates.

Plots of annual patterns for air temperature, with climatology trends for the period 1992–2020, have been computed for each lake (Figure S2 in Supplementary Material), in order to relate patterns and ranges to the cluster analysis results. When relating annual air temperature and seasonal patterns of the two turbidity clusters, cluster 1 revealed a smaller temperature range (from about 20 to 35 °C), closer to a tropical regime, with steep decrease at DOY 180–200 (i.e., monsoon rains) and then a gradual decline until the rest of the year, while cluster 2 exhibited a wider temperature range (from about 8 to 32 °C), typical of temperate/mountain regimes, with a steep decrease after DOY 280–300.

### 3.4. Comparing water quality during the dry and wet seasons in 2019

Lake Chl-a concentrations and turbidity were compared in selected periods in 2019 before (DOY 50–110), during (DOY 111–170) and after (DOY 171–230) the heatwave period, as well as during the monsoon season (DOY 231–340) (Table 3).

Among all the selected lakes, no statistical differences were found in the Chl-a concentrations when comparing the different time periods of pre, during and post-heatwave (all $p$ values $>0.05$) by ANOVA. Statistically significant differences were instead found in turbidity values in the pre-, during and post-heatwave/start of monsoon season periods ($p \leq 0.001$).

In order to investigate differences among the selected time intervals within the Chl-a and turbidity clusters, ANOVA was carried out on each cluster for the four intervals. Results are reported in Table 4 and box plots in Figure S3 in Supplementary material. Chlorophyll-a concentrations within cluster 2 were significantly different between time periods and examination of *posthoc* tests showed that for cluster 2, the period DOY 111–170 (during heatwave) was significantly different from the other periods, with Chl-a being significantly higher than in the other periods. Contrastingly, cluster 3 showed a significant difference between the latest period, which includes the monsoon and post-monsoon time window (DOY 231–240), with higher Chl-a concentrations. No significant difference between the periods could be observed in multiple comparisons of Chl-a concentrations in cluster 1, although a decrease was noted from the pre-heatwave (DOY 50–110) to the heatwave period (DOY 111–170).

For turbidity, cluster 1 showed that the examined periods were significantly different, and in particular periods DOY 111–170 (during heatwave) and 171–230 (start of monsoon season), as revealed by the *post hoc* tests. No significant differences among the considered periods were observed for cluster 2 in the performed ANOVA.

**Table 3** | Periods of comparison for the parameters Chl-a and turbidity.

| Period | DOY |
|---|---|
| Pre-heatwave | 50–110 |
| During heatwave | 111–170 |
| Post-heatwave/start monsoon | 171–230 |
| Monsoon season | 231–340 |

**Table 4** | Results of ANOVA by different clusters of chlorophyll-a and turbidity, for the four tested periods.

| Chl-a Cluster | Df | *F*-ratio | *p* |
|---|---|---|---|
| 1 | 3 | 1.51 | 0.2420 |
| 2 | 3 | 8.25 | <0.0001 |
| 3 | 3 | 4.12 | 0.0100 |
| **Turbidity cluster** | **df** | ***F*-ratio** | ***p*** |
| 1 | 3 | 9.12 | <0.0001 |
| 2 | 3 | 2.13 | 0.1100 |

Df, degrees of freedom; *F*-ratio and *p*, *p* values.

### 3.5. Cross-correlation analysis

In order to investigate correlations between time series and the strength and significance of correlations, we performed a cross-correlation analysis between monsoon cumulative rainfall (30 days) and turbidity concentrations during 2019. Although the wet/monsoon season lasts several months, the peak detection analysis showed that the rainfall timeseries is interspersed by numerous precipitation peaks. We therefore decided to relate turbidity values to cumulative rainfall during the summer monsoon season (from June to September) using cross-correlation analysis, to calculate time lags of the similarity in the two timeseries as the delay in time with one another. Results showed that the median of the time lag of the significant cross-correlation function (CCF) for all lakes was centered around zero, indicating that 30-day cumulative rainfall typically best correlates with turbidity 1 month after rainfall (Figure 7).

### 3.6. Integration of LWL

Time series for the seven lakes with LWL data available indicated that water level can vary considerably because of large freshwater withdrawal, water regulation (dams) and flooding due to monsoon precipitation and that LWL variations in reservoirs can be up to 20 m within a short period. Figure 8 shows the changes in LWL for the period 2017–2020 for three Indian lakes/reservoirs together with the 30-day cumulative precipitation and mean turbidity values for the summer monsoon period (June, July, August, September). Gandhi reservoir, which originated from the damming of the Chambal River (n. 9 in Figure 1), experienced a large drawdown in May 2019, reaching a minimum of 381 m. Following the monsoon rains, the LWL increased by 20 m (to a maximum in September-October 2019 of 401 m, Figure 8(a)) and lake water quality showed the highest value in turbidity of the 4-year period, with peaks >30 NTU in August and September 2019. Although to a lesser extent, the reservoir Lake Nath (n. 28 in Figure 1) had a major LWL variation (9 m) during 2019, with increases from a minimum of 455 m in May to a maximum of 464 m in September (Figure 8(b)). Turbidity greatly increased during the monsoon rainfall of 2019, reaching the highest values of the whole considered period with peaks >50 NTU in July and August 2019. Another example comes from a natural coastal brackish lake, Lake Chilika (n. 27 in Figure 1), which registered modest variations in LWL in 2018

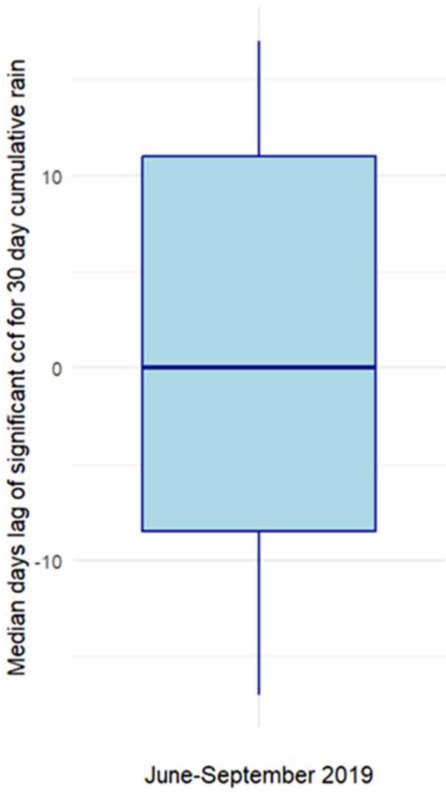


**Figure 7** | Boxplot of time lag of significant ($p \leq 0.05$) CCF (cross-correlation function) from the cross-correlation analysis between cumulative rainfall (30 days) and turbidity values.

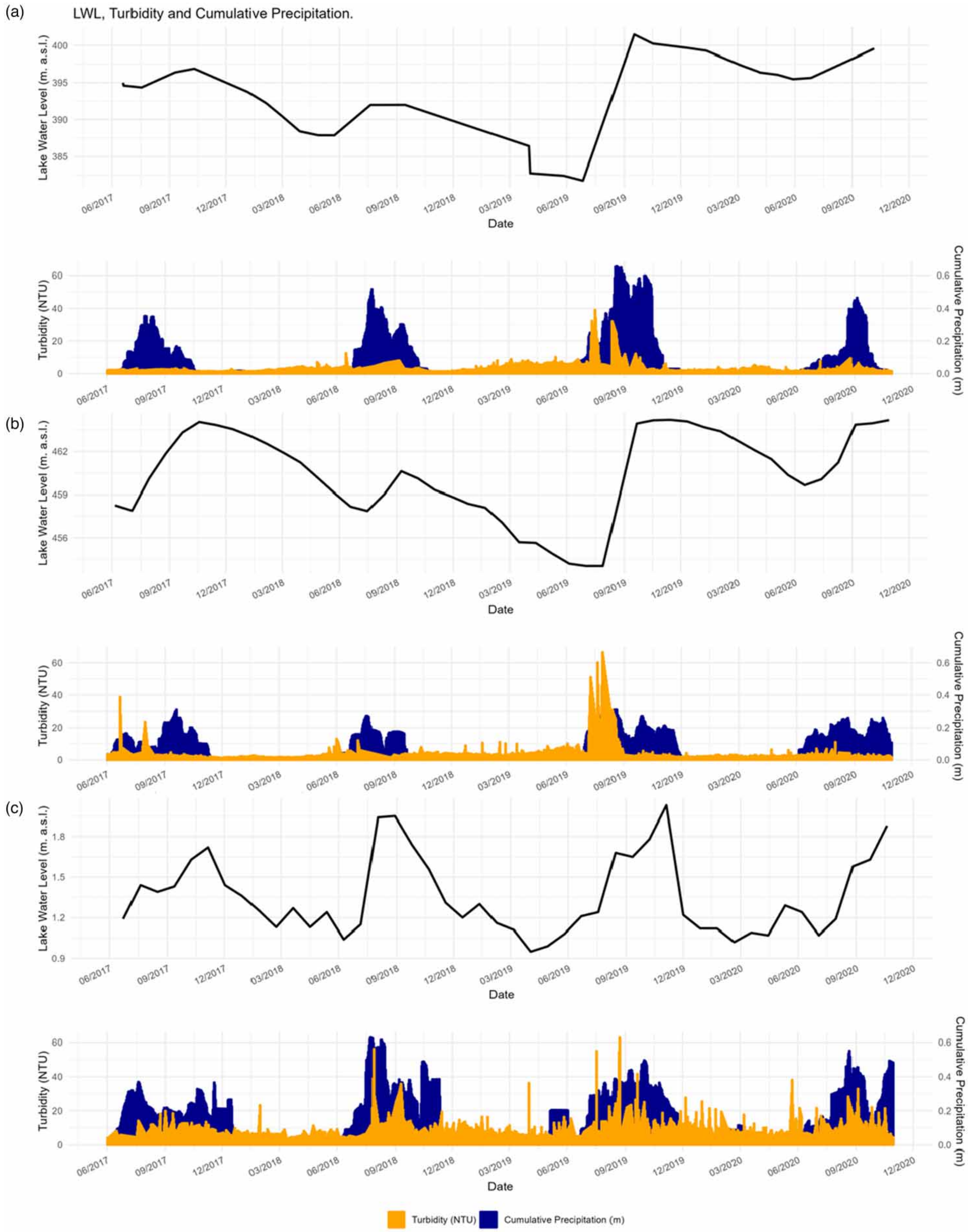


**Figure 8** | Timeseries for the period 2017–2020 of Lake Water Level (m a.s.l.; black line), 30-days cumulative precipitation (m; blue bars) and turbidity value (NTU, orange bars) for Lake Gandhi (a), Lake Nath (b), and Lake Chilika (c).

and 2019 (0.7 m), yet showed increases in turbidity after the rainfalls at comparable values during the 2 years (Figure 8(c)). In the seven lakes examined, the increase in turbidity at the start of the monsoon (DOY 171–230) was followed by a decline as the monsoon progressed (DOY 231–340). This decline was significant in ANOVA *post hoc* tests ($p < 0.05$).

## 4. DISCUSSION

This study considered patterns of lake water parameters, retrieved from satellite data, allowing a synoptic observation of water quality changes at the subcontinental scale in India. In particular, the study aimed to assess the effects of a combination of a prolonged heatwave (longer than average) and a delayed (2 weeks later) and severe monsoon (with heavier precipitation than average) that occurred during the year 2019. The delayed arrival of the southwest monsoon season contributed to prolonged critical drought conditions and water shortages in many areas with an estimated 65% of reservoirs running dry in June 2019 (Nasa Earth Observatory, https://earthobservatory.nasa.gov/images/145242/water-shortages-in-india). After the dry period, above-average monsoon rainfall caused rivers and streams to overflow, destabilizing hillsides in several regions (Nasa Earth Observatory, https://earthobservatory.nasa.gov/images/145703/unusual-monsoon-season-causes-flooding-in-india); the flood greatly affected Indian population with hundreds of people dead, more than a million displaced and extensive summer crops damaged.

### 4.1. Climatic impact on water quality and water level

LWL data indicated that 2019 was a particularly severe year for some lakes. For instance, in Lake Ghandi LWL had a variation of 19 m, with a minimum in June and rapidly increasing in the following months of July–August, when the monsoon rains replenished its waters. Moreover, both reservoirs considered for LWL in this study, Lake Gandhi and Lake Nath (Figure 8), showed that the minimum LWL reached in 2019 over the period 2017–2020 corresponded to the highest turbidity concentrations reached in the following summer (July–September) during the 4-year period. The effects of monsoon rains and floods can have a critical impact on water quality, as after an initial dilution effect, water pollutants from the watershed can cause degradation in the receiving waters (Murphy *et al.* 2018) and LWL conditions seem to play a role in determining the consequent turbidity concentration in the selected lakes. The natural shallow lake Chilika, although not suffering from large LWL variations, showed increases and peaks in turbidity with the advent of the monsoon rains likely due to both sediment runoff from the catchment and to wind-induced water mixing and sediment resuspension (Kumar *et al.* 2016; Singh *et al.* 2023).

### 4.2. Lake turbidity responses to compound weather events

When investigating water quality parameters in the present study, we found that turbidity generally slightly increased during the heatwave period and greatly increased during the monsoon season; after the monsoon period, turbidity values then decreased again. Comparing turbidity values in the different periods resulted in significant differences. This was found when analyzing the whole set of lakes, and also when differentiating in cluster 1 and cluster 2. The increase of turbidity during the monsoon period was likely due to the high sediment load from the catchment and the tributaries to the lakes, following heavy rainfalls and floodings (e.g., HaRa *et al.* 2020). Whereas the subsequent decrease in turbidity values was likely to be the result of a gradual sedimentation of particulate matter in the lakes (e.g., Mouri *et al.* 2011).

Cluster analysis performed on turbidity patterns resulted in two main clusters. Cluster 1 included the majority ($n = 25$) of the lakes considered, showing a unimodal pattern with an increasing trend in turbidity values from June and reaching maximum peaks in correspondence to the monsoon rainy season in July and August. Cluster 2 instead showed a bimodal pattern, with peaks in March and a second peak in July. Lakes' geographical and hydro-morphological features revealed that cluster 2 included lakes mainly located at higher latitudes, likely indicating that the earlier turbidity peak might be caused by snow melting processes for these lakes. An example of this cluster is Lake Tso Moriri (4,522 m asl), in the Ladakh region, with documented periods of snow coverage and occurrence of precipitation in January and February. Lake Maharana Prataph (507 m asl) and Lake Ramganga reservoir (350 m asl), although at a lower altitude, are located at the Himalayan foothills, likely receiving direct runoff from snow and glacier melting in higher regions. Previous work supports our findings, reporting that the high-altitude Tso Moriri Lake is subjected to evaporation during the dry season and supplied by snowmelt and summer monsoon precipitation (Mishra *et al.* 2015). Snowmelt indeed represents an important water input in mountainous areas, where it can significantly contribute to river discharge during flood events. This is particularly true at high-altitude catchments, as demonstrated by Goodarzi *et al.* (2023) in a case study in Northwestern Iran.

The annual pattern of turbidity in cluster 2 also showed a sharper decline during the late period of the year and reached lower values of turbidity when compared to cluster 1, likely due to a turbidity suppression due to snow presence during the winter for lakes of the Himalayan region. Air temperature patterns also confirmed a typical tropical regime with small annual temperature ranges in cluster 1 and a temperate/high mountain regime pattern with a wider range in annual air temperatures in cluster 2. In terms of LC, no particular differences were found between the two turbidity clusters, as both were dominated by cropland, although cluster 2 also included lakes with a more mixed/diverse LC. TAM indicated that the precipitation time series was more in phase with turbidity than with Chl-a, indicating a driving influence of precipitation for lake turbidity. While the influence of the monsoon rain on lake water turbidity is strong and direct, changes in Chl-a concentration reflect more interplay factors such as nutrient inputs, light availability and previous lake trophic conditions. The TAM value was, however, lowest when comparing the air temperature to precipitation, which indicates that air temperature is the variable most in phase with precipitation, as expected in the Indian subcontinent, as monsoon rainfalls induce air temperature cooling (Zhou *et al.* 2019). In addition, the results from the cross-correlation performed with cumulative precipitations and turbidity concentrations timeseries support this finding, indicating that the typical response of turbidity in our subset of Indian lakes occurred after 1 month of cumulative rain.

### 4.3. Lake chlorophyll-a dynamics

Cluster analysis performed on Chl-a patterns resulted in three main clusters. In the context of the heatwave, Chl-a either decreased (cluster 1), increased (cluster 2) or remained quite unchanged (cluster 3). When focusing on the latest period of the year, after the monsoon season, only lakes in cluster 3 showed a notable increase in Chl-a.

The decrease in Chl-a in cluster 1, which includes large and shallow lakes, during the heatwave period might be due to a decline after a previous phase of higher primary productivity, maybe related to the strong grazing and top-down control by zooplankton reaching biomass peaks in February–March in Indian shallow lakes (Malik *et al.* 2016; Verma *et al*. 2024). Alternative explanations are the lowering of the LWL due to natural water evaporation or water withdrawal for human uses. Peaks in phytoplankton biomass have been observed to occur in several south Indian lakes in the period February to May by other studies (e.g., Zafar 1986). Afterwards, Chl-a showed to remained stable with occurrences of concentration peaks, likely due to the concurrent replenishment of water and nutrients brought by the monsoon precipitations.

The increase of Chl-a during the heatwave period in cluster 2, which includes deep lakes, might be due to the establishment of thermal stratification in the water column, promoting phytoplankton blooms, possibly of cyanobacteria, in conditions of high temperature and water stratification. Phytoplankton growth might have been subsequently disrupted by increased flushing due to the arrival of monsoon rainfalls and when the water column underwent mixing conditions. It is well established that lake conditions of elevated water temperatures and water thermal stratification can lead to cyanobacteria blooms as warmer temperatures increase cyanobacteria growth rates and stratified conditions allow them to outcompete other phytoplankton species for nutrients and sunlight (Persaud *et al.* 2015). When dry periods and heatwaves are interrupted by low-pressure systems, bringing sudden declines in air and water temperatures, they can disrupt lake metabolism, leading to a rapid decline in primary production (Jeppesen *et al.* 2021). Furthermore, the concomitant rise in water turbidity could have contributed to the marked decrease in Chl-a concentrations observed in this cluster after the heatwave. Elevated turbidity levels can limit light availability in the water column, thereby constraining phytoplankton photosynthesis and subsequent growth.

The evident increase in Chl-a after the heatwave period for cluster 3, which included smaller lakes, might be due to the effects of the arrival of monsoon rainfall, bringing nutrients to the lakes by catchment runoff input and swiftly promoting primary productivity in these relatively small basins. Previous conditions during the dry season in small lakes might have seen drastic water reductions, as confirmed by data from the Global Surface Water dataset (JRC, Pekel *et al.* 2016). Moreover, a better focus on cluster 3 revealed that the increase of Chl-a was even more important during the last period of the year, after the monsoon season. Comparing turbidity values for the three Chl-a clusters in the different periods, we observed the lowest concentrations (mean 7.6 NTU) during the last period (DOY 231–240) in cluster 3, while clusters 1 and 2 reached nearly double these values (mean 13.0 NTU and mean 14.3 NTU, respectively). We thus hypothesized that in cluster 3 phytoplankton growth was enhanced by the previous period of monsoon rainfalls, bringing both water recharge and potential nutrients input to the lakes, and additionally, adequate light conditions contributed to the phytoplankton development in these lakes. In contrast, a higher level of turbidity in cluster 1 and cluster 2 might have inhibited the development of phytoplankton despite the input of potential nutrients and water recharge brought by rainfall. The increased water turbidity could have reduced light availability for phytoplankton growth, resulting in an overall Chl-a decrease, as found in other studies reporting significantly reduced lake water transparency due to surges in turbidity (e.g., Caroni *et al.* 2024). Subsequent changes in primary productivity would be mediated by both light availability and nutrient conditions, making the ultimate response of lake water Chl-a difficult to predict.

### 4.4. Implication for lake water quality

Analysis of cumulative rain and turbidity values during the period 2017–2020 highlighted that the annual variability of monsoon precipitations could influence the annual suspended sediment loads to a lake and eventually the increase in lake turbidity. Our findings are in agreement with other studies relating variability of intensity in monsoon rainfall to suspended sediment loadings in lakes under the East Asian monsoon climate (Jeon *et al.* 2017), showing that suspended sediment load is highly dependent on rainfall intensity. The extreme variation in the amount of annual precipitation is typical of the East Asian monsoon climate and can greatly influence concentrations and characteristics of the suspended sediment load to lakes. Increases in lake turbidity after monsoons have been reported in other parts of Asia. For instance, in South Korea, Kim *et al.* (2016) monitored Lake Soyang, a deep, warm, monomictic reservoir located in the Asian summer monsoon region. They found that after intensive monsoon rain events, particulate organic carbon and total phosphorus increased, and turbidity reached elevated values (>50 NTU). Their results showed that substantial amounts of inorganic nutrients and minerals were supplied to the lake by rainfall runoffs during monsoons.

Water turbidity is one of the most important water quality parameters associated with the lake ecosystem health and the provision of ecosystem services (Angradi *et al.* 2018; Stefanidis *et al.* 2023). Increased turbidity influences not only the structure and functions of lake ecosystems (Jeppesen *et al.* 1999; Hilt *et al.* 2017) impairing aquatic life and fisheries, but also has a dramatic impact on aquatic ecosystem services in water availability and quality for human consumptions (for drinking and other domestic uses), reducing water quality, blocking water supply intakes and limiting the recreational values of lakes and reservoirs (U.S. EPA 1999). In a recent review, Fabian *et al.* (2023, and references therein) found that many Asian countries need more attention in realizing that efficient water quality management is fundamental to long-term socio-economic progress.

Water quality deterioration has been influenced by recent environmental and climatic changes. In fact, the higher frequency of climatic extremes is probably worsening water quality when combined with other anthropogenic pressures such as diffuse pollution, land-use change and urbanization (Fabian *et al.* 2023). Numerous factors, such as heavy or absent precipitation, significant evapotranspiration loss, or snow melting, as well as multiple characteristics, such as intensity, duration, and timing make studying climatic extremes challenging (Brunner *et al.* 2021). Moreover, several studies on Indian lakes were carried out considering the climate conditions and variability of the monsoon rainfall of the Indo-Pacific area both at intra- and interannual scales, but less attention was put at the regional level, while the comprehension of the external forcings should be linked to regional variability (Hrudya *et al.* 2021) to better identify critical areas of climatic extreme events. Few studies have explored the impact of climate extremes on water quality in the Asian region, which is one of the most affected by climate change (Mosley 2015), with increasing pressure on lakes by severe heatwaves, extreme drawdown, higher intensity rainfall and development of phytoplankton blooms and where severe hydrological cycle changes exacerbate the region's current water management problems (Hasson *et al.* 2013).

### 4.5. Implication for adaptation and mitigation measures

The observed dynamics of lake water quality in this study highlight the urgent need to adopt both structural and non-structural (e.g., social, operational and institutional) measures to mitigate the effects of climate change in India.

To mitigate droughts associated with increasing frequency and intensity of heatwaves, as reflected in reduced lake water levels and altered ecosystem function, it becomes crucial to adopt measures such as water reuse, wetland preservation or restoration, improved irrigation efficiency and reduction of drinking water loss (e.g., by reducing leakages, building dykes and changing land-use practices) (IPCC 2014). Integrating diverse adaptation choices can enhance the overall resilience of Indian lakes and reservoirs to climate change. These should be designed with input from local communities through participatory processes and aligned with the national and regional adaptation strategies (EU 2024). An example comes from the Earthwatch India project in Bengaluru, where citizen scientists collected over 7,000 water quality data points, helping to identify risk parameters and early-warning thresholds to prevent harmful algal blooms and to guide the management of lake ecosystems to mitigate pollution and promote resilience to climate stressors (https://panorama.solutions/en/solution/monitoring-water-quality-through-citizen-science-bengaluru. Moreover, as suggested for other affected countries, such as water systems in Iran (Rezaee *et al.* 2025), climate-resilient agricultural practices such as the use of drought-resistant crops can guarantee food security in dry periods and arid conditions.

Our findings on the strong connection between enhanced turbidity and monsoonal precipitation suggest that adaptation to flooding must prioritize water quantity, water quality and flood risk management. In this regard, early-warning systems and emergency response mechanisms for extreme weather events, supported by the government, meteorological institutes and river basin authorities, will be essential. Considering the potential threats represented by an increase in lake water turbidity, particularly the deterioration of water quality for human consumption (for drinking and domestic uses), public health interventions should target improvements in water treatment infrastructure to prevent post-flood contamination risks. In this regard, nature-based solutions such as wetland restoration, reforestation and the creation of buffer zones around lakes can mitigate flood impacts by absorbing excess water and reducing flood peaks (Mitsch & Gosselink 2000; Vuik *et al.* 2018), increasing soil permeability and reducing runoff and turbidity inputs (IPCC 2014; Berland *et al.* 2017). These measures not only help stabilize water levels both in the context of droughts and floods but also support nutrient retention.

The heterogeneity of lake responses in terms of Chl-a variability confirms that localized management approaches should be preferred for maintaining ecological balance in Indian lakes under extreme environmental stressors. Such approaches include monitoring nutrient inputs from human activities, regulating land-use changes around lakes, and addressing point-source pollution to prevent eutrophication. The adaptation and mitigation strategies outlined here directly support the United Nations Sustainable Development Goals (SDGs), particularly SDG 6 'Clean Water and Sanitation' and SDG 13 'Climate Action' (UN 2015). Our findings reinforce the importance of aligning water quality and quantity management with climate adaptation policies, reinforcing the role of effective water and regional climate governance in reducing risks from floods, droughts and heatwaves (Sahani *et al.* 2019).

## 5. CONCLUSIONS

This research investigated the impacts of two compound climatic events: heatwaves and intense monsoon rainfall, on lake water quality in the Indian subcontinent using EO data. This contrasts with previous studies that have primarily focused on the effects of rising mean temperatures on inland water bodies.

One of the study's main findings was that monsoon precipitation was the main driver of water turbidity dynamics in lakes and high variation in lake water levels influenced changes in water quality. Our findings highlight the relevance of hydrological pressures on lake ecosystems, as extreme floods correlated with heavy and prolonged precipitations are projected to increase in temperate and tropical regions. Given the evidence that hydrology plays an essential role in the dynamics of lake water quality, its implications should be investigated further. In contrast, another key finding was that Chl-a patterns were more complex to explain, reflecting lake-specific factors, such as morphology, phytoplankton dynamics, and likely additional anthropogenic pressures within the catchments. These findings underline the need to consider human activities alongside climatic drivers.

The strong dependence of lake water quality and quantity on monsoon dynamics raises major management challenges under climate change. Continuous monitoring of key water quality indicators, such as turbidity and Chl-a, through satellite-based approaches offers a powerful tool for early detection of changes and timely intervention. To further enhance our understanding of lake dynamics at subcontinental scales, future research should integrate additional anthropogenic factors, including nutrient loading, water abstraction, and hydro-morphological modifications, within a regional framework.

Given the significant influence of monsoon precipitation on lake water quality and the projected changes in timing and intensity of monsoonal rains under warming scenarios, adaptive management strategies should be developed to address the variability and intensity of monsoon rains. This includes preparing for compound extremes of both droughts and floods, which are also projected to become more frequent, and implementing measures to mitigate their impacts. Lake management plans should incorporate climate change adaptation measures to enhance the resilience of lakes to extreme weather events such as heatwaves and heavy monsoon rains.

Employing satellite-derived variables from Lakes_cci provide an important, though technically demanding, opportunity to examine the response of key lake parameters, such as turbidity, Chl-a, and LWL to climatic variability across seasonal and interannual timescales. The availability of harmonized and validated observations facilitates a unique perspective on global processes, representing a considerable achievement in light of the well-known constraints of satellite remote sensing. These include spatial resolution, cloud cover and other radiometric noises that restrict observation frequency, together with long-standing technical challenges such as atmospheric correction. This study demonstrates the potential of high temporal resolution and broad spatial coverage of EO data to support lake monitoring, decision-making and policy development. These insights are crucial for developing robust and adaptive lake management strategies capable of meeting the growing challenges of climate variability and change.

## ACKNOWLEDGEMENTS

We would like to thank Clément Albergel for providing valuable feedback that supported the refinement of our analysis. We would like to acknowledge the reviewers for valuable comments and suggestions that helped improve this study.

## FUNDING

This work was supported by the Lakes_cci project (contract n. 40000125030/18/I-NB) which is part of the ESA Climate Change Initiative.

## AUTHOR CONTRIBUTIONS

R.C. and M.P. conceptualized the study, carried out the formal analysis, wrote, reviewed, and edited the article; A.J.G. carried out the formal analysis and wrote the study; M.B. and C.G. conceptualized and reviewed the study, and M.A. reviewed the study.

## DATA AVAILABILITY STATEMENT

All relevant data are available from an online repository or repositories. Satellite products from Lakes_cci project were downloaded from the Centre for Environmental Data Analysis (CEDA, https://catalogue.ceda.ac.uk/) archive within the ESA_cci Open Data Portal project framework. Lake and catchment area data were downloaded from the global HydroSHEDS database (https://www.hydrosheds.org/page/hydrolakes) and Lake-TopoCat (https://zenodo.org/records/7420810). The Köppen-Geiger climatic zones were downloaded from https://figshare.com/articles/dataset/Present_and_future_K_ppen-Geiger_climate_classification_maps_at_1-km_resolution/6396959/2. The ESA_cci Land Cover dataset (v2.1.1) was downloaded from the Climate Data Store (https://cds.climate.copernicus.eu/datasets/satellite-land-cover?tab=download). The ERA5 Land reanalysis data were downloaded from GEE (https://developers.google.com/earth-engine/datasets/catalog/ECMWF_ERA5_LAND_DAILY_AGGR?hl=it).

## CONFLICT OF INTEREST

The authors declare there is no conflict.

## REFERENCES

Albertini, C., Gioia, A., Iacobellis, V. & Manfreda, S. (2022) Detection of surface water and floods with multispectral satellites, *Remote Sensing*, **14** (23), 6005. doi:10.3390/rs14236005.

Amadori, M., Bresciani, M., Giardino, C. & Dijkstra, H. A. (2024) Slow response of surface water temperature to fast atmospheric variability reveals mixing heterogeneity in a deep lake, *Scientific Reports*, **14**, 8459. https://doi.org/10.1038/s41598-024-58547-0.

Angradi, T. R., Ringold, P. L. & Hall, K. (2018) Water clarity measures as indicators of recreational benefits provided by U.S. lakes: swimming and aesthetics, *Ecological Indicators*, **93**, 1005–1019. https://doi.org/10.1016/j.ecolind.2018.06.001.

Beck, H. E., McVicar, T. R., Vergopolan, N., Berg, A., Lutsko, N. J., Dufour, A., Zeng, Z., Jiang, X., van Dijk, A. I. J. M. & Miralles, D. G. (2023) High-resolution (1 km) Köppen-Geiger maps for 1901–2099 based on constrained CMIP6 projections, *Scientific Data*, **10** (1), 724. doi:10.1038/s41597-023-02549-6.

Berland, A., Shiflett, S. A., Shuster, W. D., Garmestani, A. S., Goddard, H. C., Herrmann, D. L. & Hopton, M. E. (2017) The role of trees in urban stormwater management, *Landscape and Urban Planning*, **162**, 167–177. doi:10.1016/j.landurbplan.2017.02.017.

Blunden, J. & Arndt, D. S. (eds.) (2020) State of the climate in 2019, *Bulletin of the American Meteorological Society*, **101** (8), S1–S429.. https://doi.org/10.1175/2020BAMSStateoftheClimate.1.

Brunner, M. I., Slater, L., Tallaksen, L. M. & Clark, M. (2021) Challenges in modeling and predicting floods and droughts: a review, *Wiley Interdisciplinary Reviews: Water*, **8** (3), e1520. doi:10.1002/wat2.1520.

Caretta, M. A., Mukherji, A., Arfanuzzaman, M., Betts, R. A., Gelfan, A., Supratid, S., Hirabayashi, Y., Lissner, T. K., Liu, J., Lopez Gunn, E., Morgan, R., Mwanga, S. & Supratid, S. (2022) Water. In: Pörtner, H.-O., Roberts, D. C., Tignor, M., Poloczanska, E. S., Mintenbeck, K., Alegría, A., Craig, M., Langsdorf, S., Löschke, S., Möller, V., Okem, A. & Rama, B. (eds.) *Climate Change 2022: Impacts, Adaptation and Vulnerability. Contribution of Working Group II to the Sixth Assessment Report of the Intergovernmental Panel on Climate Change*. Cambridge, UK: Cambridge University Press and New York, NY, USA, pp. 551–712. doi:10.1017/9781009325844.006.

Caroni, R., Pinardi, M., Free, G., Stroppiana, D., Parigi, L., Tellina, G., Bresciani, M., Albergel, C. & Giardino, C. (2024) Investigating the impact of wildfires on lake water quality using earth observations, *Applied Sciences*, **14**, 2626. doi:10.3390/app14062626.

Carrea, L., Crétaux, J. F., Liu, X., Wu, Y., Calmettes, B., Duguay, C. R., Merchant, C. J., Selmes, N., Simis, S. G. H., Warren, M., Yesou, H., Müller, D., Jiang, D., Embury, O., Bergé-Nguyen, M. & Albergel, C. (2023) Satellite-derived multivariate world-wide lake physical variable timeseries for climate studies, *Scientific Data*, **10** (1), 30. doi:10.1038/s41597-022-01889-z.

Collins, M., Beverley, J. D., Bracegirdle, T. J., Catto, J., McCrystall, M., Dittus, A., Freychet, N., Grist, J., Hegerl, G. C., Holland, P. R., Holmes, C., Josey, S. A., Joshi, M., Hawkins, E., Lo, E., Lord, N., Mitchell, D., Monerie, P.-A., Priestley, M. D. K., Scaife, A., Screen, J., Senior, N., Sexton, D., Shuckburgh, E., Siegert, S., Simpson, C., Stephenson, D. B., Sutton, R., Thompson, V., Wilcox, L. J. & Woollings, T. (2024) Emerging signals of climate change from the equator to the poles: new insights into a warming world, *Frontiers in Science*, **2**, 1340323. doi:10.3389/fsci.2024.1340323.

Crétaux, J. F. & Birkett, C. (2006) Lake studies from satellite radar altimetry, *Comptes Rendus Geoscience*, **338** (14-15), 1098–1112.

Defourny, P., Lamarche, C., Brockmann, C., Boettcher, M., Bontemps, S., De Maet, T., Duveiller, G., Harper, K., Hartley, A., Kirches, G., Moreau, I., Peylin, P., Ottlé, C., Radoux, J., Van Bogaert, E., Ramoino, F., Albergel, C. & Arino, O. (2023) *Observed Annual Global Land-use Change From 1992 to 2020 Three Times More Dynamic Than Reported by Inventory-Based Statistics*. In preparation. Available at: http://maps.elie.ucl.ac.be/CCI/viewer/download.php (Accessed 2025).

Ding, T., Qian, W. & Yan, Z. (2010) Changes in hot days and heat waves in China during 1961–2007, *International Journal of Climatology*, **30** (10), 1452–1462. doi:10.1002/joc.1989.

Dosio, A. & Fischer, E. M. (2018) Will half a degree make a difference? robust projections of indices of mean and extreme climate in Europe under 1.5 C, 2 C, and 3 C global warming, *Geophysical Research Letters*, **45** (2), 935–944. doi:10.1002/2017GL076222.

Dube, A., Singh, H. & Ashrit, R. (2021) Heat waves in India during MAM 2019: verification of ensemble based probabilistic forecasts and impact of bias correction, *Atmospheric Research*, **251**, 105421. doi:10.1016/j.atmosres.2020.105421.

Dunn, R. J. H., Stanitski, D. M., Gobron, N. & Willett, K. M. (eds.) (2020) Global climate [in "State of the climate in 2019"], *Bulletin of the American Meteorological Society*, **101** (8), S9–S127. https://doi.org/10.1175/BAMSD-20-0104.1.

European Commission: Directorate-General for Environment (2024) *River Basin Management in A Changing Climate – Common Implementation Strategy for the Water Framework Directive and the Floods Directive*. Luxembourg: Publications Office of the European Union. Available at: https://data.europa.eu/doi/10.2779/126657.

Fabian, P. S., Kwon, H. H., Vithanage, M. & Lee, J. H. (2023) Modeling, challenges, and strategies for understanding impacts of climate extremes (droughts and floods) on water quality in Asia: a review, *Environmental Research*, **225**, 115617. doi:10.1016/j.envres.2023.115617.

Folgado, D., Barandas, M., Matias, R., Martins, R., Carvalho, M. & Gamboa, H. (2018) Time alignment measurement for time series, *Pattern Recognition*, **81**, 268–279. doi:10.1016/j.patcog.2018.04.003.

Free, G., Bresciani, M., Pinardi, M., Simis, S., Liu, X., Albergel, C. & Giardino, C. (2022) Investigating lake chlorophyll-a responses to the 2019 European double heatwave using satellite remote sensing, *Ecological Indicators*, **142**, 109217. doi:10.1016/j.ecolind.2022.109217.

Goodarzi, M. R., Sabaghzadeh, M. & Niazkar, M. (2023) Evaluation of snowmelt impacts on flood flows based on remote sensing using SRM model, *Water*, **15** (9), 1650. doi:10.3390/w15091650.

Habeeb, D., Vargo, J. & Stone Jr, B. (2015) Rising heat wave trends in large US cities, *Natural Hazards*, **76** (3), 1651–1665.

HaRa, J., Atique, U. & An, K. G. (2020) Multiyear links between water chemistry, algal chlorophyll, drought-flood regime, and nutrient enrichment in a morphologically complex reservoir, *International Journal of Environmental Research and Public Health*, **17** (9), 3139. doi:10.3390/ijerph17093139.

Hari, V., Ghosh, S., Zhang, W. & Kumar, R. (2022) Strong influence of north Pacific Ocean variability on Indian summer heatwaves, *Nature Communications*, **13** (1), 5349. doi:10.1038/s41467-022-32942-5.

Hasson, S., Lucarini, V. & Pascale, S. (2013) Hydrological cycle over south and southeast Asian river basins as simulated by PCMDI/CMIP3 experiments, *Earth System Dynamics*, **4** (2), 199–217. doi:10.5194/esd-4-199-2013.

Hilt, S., Brothers, S., Jeppesen, E., Veraart, A. J. & Kosten, S. (2017) Translating regime shifts in shallow lakes into changes in ecosystem functions and services, *Bioscience*, **67**, 928–936. https://doi.org/10.1093/biosci/bix106.

Hrudya, P. H., Varikoden, H. & Vishnu, R. (2021) A review on the Indian summer monsoon rainfall, variability and its association with ENSO and IOD, *Meteorology and Atmospheric Physics*, **133**, 1–14. doi:10.1007/s00703-020-00734-5.

Huang, X., Zhou, T., Turner, A., Dai, A., Chen, X., Clark, R., Jiang, J., Man, W., Murphy, J., Rostron, J., Wu, B., Zhang, L., Zhang, W. & Zou, L. (2020) The recent decline and recovery of Indian summer monsoon rainfall: relative roles of external forcing and internal variability, *Journal of Climate*, **33** (12), 5035–5060. doi:10.1175/JCLI-D-19-0833.1.

Hyndman, R. J. & Khandakar, Y. (2008) Automatic time series forecasting: the forecast package for R, *Journal of Statistical Software*, **27** (3), 1–22. doi:10.18637/jss.v027.i03.

Indian Meteorological Department (2020) *Annual Report 2019*. New Delhi – 110 003 (India): Information Science & Knowledge Resource Development Division (IS&KRDD) (Formerly Publication Section) India Meteorological Department.

IPCC (2013) Chapter 12: Long-term Climate Change: Projections, Commitments and Irreversibility. In: Stocker, T. F., Qin, D., Plattner, G.-K., Tignor, M., Allen, S. K., Boschung, J., Nauels, A., Xia, Y., Bex, V. & Midgley, P. M. (eds.) *Climate Change 2013: the Physical Science Basis. Contribution of Working Group I to the Fifth Assessment Report of the Intergovernmental Panel on Climate Change*. Cambridge, UK: Cambridge University Press and New York, NY, USA, pp. 1029–1136.

IPCC (2014) In: Pachauri, R. K. & Meyer, L. A. (eds.) Section 4.3: Future risks and opportunities, adaptation and mitigation. *Climate Change 2014: Synthesis Report. Contribution of Working Groups I, II and III to the Fifth Assessment Report of the Intergovernmental Panel on Climate Change*. Geneva, Switzerland: IPCC, pp. 79–104.

Jeon, J. H., Park, C. G., Choi, D. & Kim, T. (2017) Characteristics of suspended sediment loadings under Asian summer monsoon climate using the hydrological simulation program-FORTRAN, *Sustainability*, **9** (1), 44. https://doi.org/10.3390/su9010044.

Jeppesen, E., Jensen, J. P., Søndergaard, M. & Lauridsen, T. (1999) Trophic dynamics in turbid and clearwater lakes with special emphasis on the role of zooplankton for water clarity. In: Walz, N. & Nixdorf, B. (eds.) *Shallow Lakes' 98: Trophic Interactions in Shallow Freshwater and Brackish Waterbodies*, Dordrecht, Netherlands: Springer, pp. 217–231.

Jeppesen, E., Audet, J., Davidson, T. A., Neif, E. M., Cao, Y., Filiz, N., Lauridsen, T., Larsen, S., Beklioğlu, M., Sh, T. & Søndergaard, M. (2021) Nutrient loading, temperature and heat wave effects on nutrients, oxygen and metabolism in shallow lake mesocosms pre-adapted for 11 years, *Water*, **13** (2), 127. doi:10.3390/w13020127.

Jiao, T., Williams, C. A., De Kauwe, M. G., Schwalm, C. R. & Medlyn, B. E. (2021) Patterns of post-drought recovery are strongly influenced by drought duration, frequency, post-drought wetness, and bioclimatic setting, *Global Change Biology*, **27** (19), 4630–4643.

Jin, Q. & Wang, C. (2017) A revival of Indian summer monsoon rainfall since 2002, *Nature Climate Change*, **7** (8), 587–594. doi:10.1038/nclimate3348.

Joehnk, K. D., Huisman, J. E. F., Sharples, J., Sommeijer, B. E. N., Visser, P. M. & Stroom, J. M. (2008) Summer heatwaves promote blooms of harmful cyanobacteria, *Global Change Biology*, **14** (3), 495–512. doi:10.1111/j.1365-2486.2007.01510.x.

Joyce, K. E., Belliss, S. E., Samsonov, S. V., McNeill, S. J. & Glassey, P. J. (2009) A review of the status of satellite remote sensing and image processing techniques for mapping natural hazards and disasters, *Progress in Physical Geography: Earth and Environment*, **33**, 183–207. doi:10.1177/0309133309339563.

Kansakar, P. & Hossain, F. (2016) A review of applications of satellite earth observation data for global societal benefit and stewardship of planet earth, *Space Policy*, **36**, 46–54. doi:10.1016/j.spacepol.2016.05.005.

Kassambara, A. & Mundt, F. (2017) Package 'factoextra', *Extract and Visualize the Results of Multivariate Data Analyses*, **76** (2), 10–8637.

Kim, K., Kim, B., Knorr, K. H., Eum, J., Choi, Y., Jung, S. & Peiffer, S. (2016) Potential effects of sediment processes on water quality of an artificial reservoir in the Asian monsoon region, *Inland Waters*, **6** (3), 423–435. doi:10.1080/IW-6.3.852.

Kumar, A., Equeenuddin, S. M., Mishra, D. R. & Acharya, B. C. (2016) Remote monitoring of sediment dynamics in a coastal lagoon: long-term spatio-temporal variability of suspended sediment in Chilika, *Estuarine, Coastal and Shelf Science*, **170**, 155–172. doi:10.1016/j.ecss.2016.01.018.

Kumar, P., Srivastava, S. S., Jivani, N., Varma, A. K., Yokoyama, C. & Kubota, T. (2024) Long-term assessment of ERA5 reanalysis rainfall for lightning events over India observed by tropical rainfall measurement mission lightning imaging sensor, *Quarterly Journal of the Royal Meteorological Society*, **150** (761), 2472–2488.

Maechler, M., Rousseeuw, P., Struyf, A., Hubert, M. & Hornik, K. (2024) *Cluster: Cluster Analysis Basics and Extensions*. R package version 2.1.8 – For new features, see the 'NEWS' and the 'Changelog' file in the package source). Vienna, Austria: R Foundation for Statistical Computing. Available at: https://CRAN.R-project.org/package=cluster.

Malik, M., Balkhi, M. H., Abubakr, A. & Bhat, B. A. (2016) Qualitative and quantitative studies of *Rotifera* as indices of water quality in Dal lake, Kashmir, *Ecology, Environment and Conservation*, **22** (4), 379–385.

Meehl, G. A. & Tebaldi, C. (2004) More intense, more frequent, and longer lasting heat waves in the 21st century, *Science*, **305** (5686), 994–997. doi:10.1126/science.1098704.

Messager, M. L., Lehner, B., Grill, G., Nedeva, I. & Schmitt, O. (2016) Estimating the volume and age of water stored in global lakes using a geo-statistical approach, *Nature Communications*, **7**, 13603. https://doi.org/10.1038/ncomms13603.

Mishra, P. K., Anoop, A., Schettler, G., Prasad, S., Jehangir, A., Menzel, P., Naumann, R., Yousuf, A. R., Basavaiah, N., Deenadayalan, K., Wiesner, M. G. & Gaye, B. (2015) Reconstructed late Quaternary hydrological changes from Lake Tso Moriri, NW Himalaya, *Quaternary International*, 371, 76–86.

Mitsch, W. J. & Gosselink, J. G. (2000) The value of wetlands: importance of scale and landscape setting, *Ecological Economics*, **35** (1), 25–33. doi:10.1016/S0921-8009(00)00165-8.

Mosley, L. M. (2015) Drought impacts on the water quality of freshwater systems; review and integration, *Earth-Science Reviews*, **140**, 203–214. doi:10.1016/j.earscirev.2014.11.010.

Mouri, G., Shiiba, M., Hori, T. & Oki, T. (2011) Modeling reservoir sedimentation associated with an extreme flood and sediment flux in a mountainous granitoid catchment, Japan, *Geomorphology*, **125** (2), 263–270. https://doi.org/10.1016/j. geomorph.2010.09.026.

Muñoz Sabater, J. (2019) *ERA5-Land Monthly Averaged Data From 1981 to Present*. Copernicus Climate Change Service (C3S) Climate Data Store (CDS). Reading, United Kingdom: European Centre for Medium-Range Weather Forecasts (ECMWF). [Accessed: February 2025], doi:10.24381/cds.68d2bb30.

Muñoz-Sabater, J., Dutra, E., Agustí-Panareda, A., Albergel, C., Arduini, G., Balsamo, G., Boussetta, S., Choulga, M., Harrigan, S., Hersbach, H., Martens, B., Miralles, D. G., Piles, M., Rodríguez-Fernández, N. J., Zsoter, E., Buontempo, C. & Thépaut, N. J. (2021) ERA5-Land: a state-of-the-art global reanalysis dataset for land applications, *Earth System Science Data*, **13** (9), 4349–4383. doi:10.5194/essd-13-4349-2021.

Murphy, S. F., McCleskey, R. B., Martin, D. A., Writer, J. H. & Ebel, B. A. (2018) Fire, flood, and drought: extreme climate events alter flow paths and stream chemistry, *Journal of Geophysical Research: Biogeosciences*, **123** (8), 2513–2526. https://doi.org/10.1029/2017JG004349.

Neil, C., Spyrakos, E., Hunter, P. & Tyler, A. (2019) A global approach for chlorophyll-a retrieval across optically complex inland waters based on optical water types, *Remote Sensing of Environment*, **229**, 159–178. https://doi.org/10.1016/j.rse.2019.04.027.

NOAA National Centers for Environmental Information (2019) *Monthly Global Climate Report for Annual 2019*. Asheville, NC, USA: National Oceanic and Atmospheric Administration. published online January 2020, retrieved on September 5, 2025. Available at: https://www.ncei.noaa.gov/access/monitoring/monthly-report/global/201913.

Organisation for Economic Cooperation and Development, (OECD) (1982) *Eutrophication of Waters: Monitoring, Assessment and Control*. Paris, France: OECD.

Parmesan, C., Morecroft, M. D., Trisurat, Y., Adrian, R., Anshari, G. Z., Talukdarr, G. H., (2022) Terrestrial and Freshwater Ecosystems and Their Services. In: Pörtner, H.-O., Roberts, D. C., Tignor, M., Poloczanska, E. S., Mintenbeck, K., Alegría, A., Craig, M., Langsdorf, S., Löschke, S., Möller, V., Okem, A. & Rama, B. (eds.) *Climate Change 2022: Impacts, Adaptation and Vulnerability. Contribution of Working Group II to the Sixth Assessment Report of the Intergovernmental Panel on Climate Change*. Cambridge, UK: Cambridge University Press and New York, NY, USA, pp. 197–377.

Pekel, J. F., Cottam, A., Gorelick, N. & Belward, A. S. (2016) High-resolution mapping of global surface water and its long-term changes, *Nature*, **540** (7633), 418–422. doi:10.1038/nature20584.

Perkins, S. E. & Alexander, L. V. (2013) On the measurement of heat waves, *Journal of Climate*, **26** (13), 4500–4517. doi:10.1175/JCLI-D-12-00383.1.

Perkins-Kirkpatrick, S. E. & Lewis, S. C. (2020) Increasing trends in regional heatwaves, *Nature Communications*, **11** (1), 3357. doi:10.1038/s41467-020-16970-7.

Persaud, A. D., Paterson, A. M., Dillon, P. J., Winter, J. G., Palmer, M. & Somers, K. M. (2015) Forecasting cyanobacteria dominance in Canadian temperate lakes, *Journal of Environmental Management*, **151**, 343–352. doi:10.1016/j.jenvman.2015.01.009.

Pinardi, M., Stroppiana, D., Caroni, R., Parigi, L., Tellina, G., Free, G., Giardino, C., Albergel, C. & Bresciani, M. (2023) Assessing the impact of wildfires on water quality using satellite remote sensing: the Lake Baikal case study, *Frontiers in Remote Sensing*, **4**, 1107275. doi:10.3389/frsen.2023.1107275.

Rasconi, S., Winter, K. & Kainz, M. J. (2017) Temperature increase and fluctuation induce phytoplankton biodiversity loss–Evidence from a multi-seasonal mesocosm experiment, *Ecology and Evolution*, **7** (9), 2936–2946. doi:10.1002/ece3.2889.

Ratnam, J. V., Behera, S. K., Ratna, S. B., Rajeevan, M. & Yamagata, T. (2016) Anatomy of Indian heatwaves, *Scientific Reports*, **6**, 24395. doi:10.1038/srep24395.

R Core Team (2021) *R: A Language and Environment for Statistical Computing*. Vienna, Austria: R Foundation for Statistical Computing. Available at: https://www.R-project.org/.

Rezaee, A., Goodarzi, M. R., Etemadfard, H. & Alavizadeh, M. (2025) A copula-based framework for assessing heat wave extremes and probability of occurrence in Iran: implications for climate change, *Stochastic Environmental Research and Risk Assessment*, **39**, 2461–2477. https://doi.org/10.1007/s00477-025-02979-1.

Rohini, P., Rajeevan, M. & Srivastava, A. K. (2016) On the variability and increasing trends of heat waves over India, *Scientific Reports*, **6**, 1–9. doi:10.1038/srep26153.

Roxy, M. K. (2017) Land warming revives monsoon, *Nature Climate Change*, **7** (8), 549–550. doi:10.1038/nclimate3356.

Sahani, J., Kumar, P., Debele, S., Spyrou, C., Loupis, M., Aragão, L., Porcù, F., Shah, M. A. R. & Di Sabatino, S. (2019) Hydro-meteorological risk assessment methods and management by nature-based solutions, *Science of the Total Environment*, **696**, 133936. doi:10.1016/j.scitotenv.2019.133936.

Sauter, C., Fowler, H. J., Westra, S., Ali, H., Peleg, N. & White, C. J. (2023) Compound extreme hourly rainfall preconditioned by heatwaves most likely in the mid-latitudes, *Weather and Climate Extremes*, **40**, 100563. doi:10.1016/j.wace.2023.100563.

Seneviratne, S. I., Zhang, X., Adnan, M., Badi, W., Dereczynski, C., Di Luca, A., Ghosh, S., Iskandar, I., Kossin, J., Lewis, S., Otto, F., Pinto, I., Satoh, M., Vicente-Serrano, S. M., Wehner, M. & Zhou, B. (2021) Weather and Climate Extreme Events in a Changing Climate. In: Masson-Delmotte, V., Zhai, P., Pirani, A. & Connors, S. L., & Zhou, B. (eds.) *Climate Change 2021: the Physical Science Basis. Contribution of Working Group I to the Sixth Assessment Report of the Intergovernmental Panel on Climate Change*. Cambridge, UK: Cambridge University Press and New York, NY, USA, pp. 1513–1766.

Shaw, R., Luo, Y., Cheong, T. S., Abdul Halim, S., Chaturvedi, S., Hashizume, M., Insarov, G. E., Ishikawa, Y., Jafari, M., Kitoh, A., Pulhin, J., Singh, C., Vasant, K., Zhang, Z., (2022) Asia. In: Pörtner, H.-O., Roberts, D. C., Tignor, M., Poloczanska, E. S., Mintenbeck, K., Alegría, A., Craig, M., Langsdorf, S., Löschke, S., Möller, V., Okem, A. & Rama, B. (eds.) *Climate Change 2022: Impacts, Adaptation and Vulnerability. Contribution of Working Group II to the Sixth Assessment Report of the Intergovernmental Panel on Climate Change*. Cambridge, UK: Cambridge University Press and New York, NY, USA, pp. 1457–1579. doi:10.1017/9781009325844.012.

Sikder, M. S., Wang, J., Allen, G. H., Sheng, Y., Yamazaki, D., Song, C., Ding, M., Crétaux, J.-F. & Pavelsky, T. M. (2023) Lake-TopoCat: a global lake drainage topology and catchment database, *Earth System Science Data*, **15**, 3483–3511. https://doi.org/10.5194/essd-15-3483-2023.

Simis, S., Carrea, L., Calmettes, B., Crétaux, J.-F., Duguay, C., Liu, X., Mangilli, A., Müller, D. & Yésou, H. (2023) *Lakes Climate Change Initiative Algorithm Theoretical Basis Document (ATBD), Version 2.1.1*. Paris, France: European Space Agency.

Singh, A. K., Tripathi, J. N., Kotlia, B. S., Singh, K. K. & Kumar, A. (2019) Monitoring groundwater fluctuations over India during Indian summer monsoon (ISM) and northeast monsoon using GRACE satellite: impact on agriculture, *Quaternary International*, **507**, 342–351. doi:10.1016/j.quaint.2018.10.036.

Singh, S., Stefanidis, K. & Mishra, P. K. (2023) Morphometric study of lake basins from the Indian subcontinent: a critical review, *Journal of Earth System Science*, **132** (1), 29. doi:10.1007/s12040-022-02030-9.

Smale, D. A., Wernberg, T., Oliver, E. C., Thomsen, M., Harvey, B. P., Straub, S. C., Burrows, M. T., Alexander, L. V., Benthuysen, J. A., Donat, M. G., Feng, M., Hobday, A. J., Holbrook, N. J., Perkins-Kirkpatrick, S. E., Scannell, H. A., Sen Gupta, A., Payne, B. L. & Moore, P. J. (2019) Marine heatwaves threaten global biodiversity and the provision of ecosystem services, *Nature Climate Change*, **9** (4), 306–312. https://doi.org/10.1038/s41558-019-0412-1.

Soetaert, K. (2021) *plot3D: Plotting Multi-Dimensional Data*. R package version 1.4. Vienna, Austria: R Foundation for Statistical Computing. Available at: http://CRAN.R-project.org/package=plot3D.

Stefanidis, K., Varlas, G., Papaioannou, G., Papadopoulos, A. & Dimitriou, E. (2023) Assessing temporal variability of lake turbidity and trophic state of European lakes using open data repositories, *Science of The Total Environment*, **857**, 159618. doi:10.1016/j.scitotenv.2022.159618.

Stockwell, J. D., Doubek, J. P., Adrian, R., Anneville, O., Carey, C. C., Carvalho, L., De Senerpont Domis, L. N., Dur, G., Frassl, M. A., Grossart, H., Ibelings, B. W., Lajeunesse, M. J., Lewandowska, A. M., Llames, M. E., Matsuzaki, S. S., Nodine, E. R., Nõges, P., Patil, V. P., Pomati, F., Rinke, K., Rudstam, L. G., Rusak, J. A., Salmaso, N., Seltmann, C. T., Straile, D., Thackeray, S. J., Thiery, W., Urrutia-Cordero, P., Venail, P., Verburg, P., Woolway, R. I., Zohary, T., Andersen, M. R., Bhattacharya, R., Hejzlar, J., Janatian, N., Kpodonu, A. T. N. K., Williamson, T. J. & Wilson, H. L. (2020) Storm impacts on phytoplankton community dynamics in lakes, *Global Change Biology*, **26** (5), 2756–2784. doi:10.1111/gcb.15033.

Straub, S. C., Wernberg, T., Thomsen, M. S., Moore, P. J., Burrows, M. T., Harvey, B. P. & Smale, D. A. (2019) Resistance, extinction, and everything in between – the diverse responses of seaweeds to marine heatwaves, *Frontiers in Marine Science*, **6**, 763. doi: 10.3389/fmars.2019.00763.

Szekely, G. J. & Rizzo, M. L. (2005) Hierarchical clustering via joint between-within distances: extending ward's minimum variance method, *Journal of Classification*, **22** (2), 151–184. doi:10.1007/s00357-005-0012-9.

Thornton, P. K., Ericksen, P. J., Herrero, M. & Challinor, A. J. (2014) Climate variability and vulnerability to climate change: a review, *Global Change Biology*, **20**, 3313–3328. https://doi.org/10.1111/gcb.12581.

Till, A., Rypel, A. L., Bray, A. & Fey, S. B. (2019) Fish die-offs are concurrent with thermal extremes in north temperate lakes, *Nature Climate Change*, **9** (8), 637–641. doi:10.1038/s41558-019-0520-y.

UN (2015) *Transforming Our World: the 2030 Agenda for Sustainable Development*. Resolution Adopted by the General Assembly on 25 September 2015, 42809, New York, USA: United Nations, pp. 1–13. https://doi.org/10.1007/s13398-014-0173-7.2.

U.S. Environmental Protection Agency (EPA) (1999) *EPA 841-B-99-004 Protocol for Developing Sediment TMDLs*, 1st edn. Washington, DC, USA: U.S. EPA.

Verma, S., Singh, G., Singh, A., Ravikant, K., Mehta, P., Maurya, M. & Pandey, S. (2024) Assessment of plankton diversity of blue bird lake at Hisar Haryana, India, *International Journal of Advanced Biochemistry Research*, **SP-8** (1), 77–86. doi:10.33545/26174693.2024.v8.i1Sb.288.

Vittal, H., Villarini, G. & Zhang, W. (2020a) On the role of the Atlantic Ocean in exacerbating Indian heat waves, *Climate Dynamics*, **54** (3), 1887–1896. doi:10.1007/s00382-019-05093-5.

Vittal, H., Karmakar, S., Ghosh, S. & Murtugudde, R. (2020b) A comprehensive India-wide social vulnerability analysis: highlighting its influence on hydro-climatic risk, *Environmental Research Letters*, **15** (1), 014005. doi:10.1088/1748-9326/ab6499.

Vuik, V., Van Vuren, S., Borsje, B. W., van Wesenbeeck, B. K. & Jonkman, S. N. (2018) Assessing safety of nature-based flood defenses: dealing with extremes and uncertainties, *Coastal Engineering*, **139**, 47–64. doi:10.1016/j.coastaleng.2018.05.002.

Wickham, H. (2016) *ggplot2: Elegant Graphics for Data Analysis*. New York: Springer-Verlag. ISBN 978-3-319-24277-4. Available at: https://ggplot2.tidyverse.org.

Woolway, R. I., Jennings, E., Shatwell, T., Golub, M., Pierson, D. C. & Maberly, S. C. (2021) Lake heatwaves under climate change, *Nature*, **589** (7842), 402–407. doi:10.1038/s41586-020-03119-1.

Woolway, R. I., Sharma, S. & Smol, J. P. (2022a) Lakes in hot water: the impacts of a changing climate on aquatic ecosystems, *Bioscience*, **72** (11), 1050–1061. doi:10.1093/biosci/biac052.

Woolway, R. I., Albergel, C., Frölicher, T. L. & Perroud, M. (2022b) Severe lake heatwaves attributable to human-induced global warming, *Geophysical Research Letters*, **49**, e2021GL097031. https://doi. org/10.1029/2021GL097031.

Yang, Y. & Yuan, C. (2025) Causality of compound extreme heat-precipitation events in northeastern China, *Atmospheric Research*, **316**, 107975. doi:10.1016/j.atmosres.2025.107975.

Yang, J., Gong, P., Fu, R., Zhang, M., Chen, J., Liang, S., Xu, B., Shi, J. & Dickinson, R. (2013) The role of satellite remote sensing in climate change studies, *Nature Climate Change*, **3** (10), 875–883. doi:10.1038/nclimate1908.

You, J. & Wang, S. (2021) Higher probability of occurrence of hotter and shorter heat waves followed by heavy rainfall, *Geophysical Research Letters*, **48** (17), e2021GL094831. doi:10.1029/2021GL094831.

Zafar, A. R. (1986) Seasonality of phytoplankton in some south Indian lakes, *Hydrobiologia*, **138**, 177–187. doi:10.1007/BF00027239.

Zeileis, A., Grothendieck, G., Ryan, J. A., Ulrich, J. M. & Andrews, F. (2022) *Zoo: s3 Infrastructure for Regular and Irregular Time Series (Z's Ordered Observations), R Package Version 1.8-10*. Vienna, Austria: R Foundation for Statistical Computing.

Zhao, S., Liu, M., Tao, M., Zhou, W., Lu, X., Xiong, Y., Li, F. & Wang, Q. (2023) The role of satellite remote sensing in mitigating and adapting to global climate change, *Science of the Total Environment*, **904**, 166820. doi:10.1016/j.scitotenv.2023.166820.

Zhou, Z. Q., Xie, S. P. & Zhang, R. (2019) Variability and predictability of Indian rainfall during the monsoon onset month of June, *Geophysical Research Letters*, **46** (24), 14782–14788. doi:10.1029/2019GL085495.

Zore, T., Landu, K., Gogoi, P. P. & Vinoj, V. (2021) Effect of tropical sub-seasonal variability on heatwaves over India, *International Journal of Climatology*, **41** (Suppl. 1), E2258–E2268.

First received 24 April 2025; accepted in revised form 25 September 2025. Available online 15 October 2025